Muscarinic acetylcholine receptors in congestive heart failure - a receptor binding study

Thesis for the *cand.pharm.* degree in pharmacology

by Anette Glende

Department of Pharmacology
Faculty of Medicine
University of Oslo

School of Pharmacy
Faculty of Mathematics and Natural Sciences
University of Oslo
2004

Acknowledgements

This study has been carried out at the Department of Pharmacology, University of Oslo from November 2003 until November 2004 under the supervision of professor *dr.med* Tor Skomedal, professor *dr.med* Jan Bjørn Osnes and professor *dr.med* Finn Olav Levy. I wish to thank the Department of Pharmacology for providing the resources necessary to accomplish the present study.

First I specially want to show my deepest gratitude to my supervisors professor *dr.med* Tor Skomedal and professor *dr.med* Jan-Bjørn Osnes for sharing their knowledge, enthusiasm and great support during my time in their group.

I would also like to thank professor *dr.med* Finn Olav Levy for advices and support.

Thanks to Kurt Krobert for interesting discussions, advice and help. Also, thanks to Kjetil Wessel Andressen, Jens Henrik Norum and Eirik Qvigstad for kind help when needed. Thanks to Faraz Afzal and Rizwan Hussain for supplying ventricles from normal hearts. I would also like to thank Iwona Schiander for technical help in the lab and friendly support during the year.

Thanks to Institute for Experimental Medical Research, Ullevål University Hospital (Research group of professor Ole M. Sejersted) for providing failing and non-failing hearts.

Oslo, November 2004 Anette Glende

Table of contents

Abbreviations

Abbreviation	Full name
AC	Adenylyl cyclase
AChR	Acetylcholine receptor
ANP	Atrial natriuretic peptide
AR	Adrenoceptor
α-AR	α-adrenoceptor
β-AR	β-adrenoceptor
BCA	Bicinchoninic acid
cAMP	Cyclic 3´,5´-adenosine monophosphate
CCh	Carbachol
CHF	Congestive heart failure
DAG	Diacylglycerol
EDTA	Ethylenedinitrilo tetraacetic acid
F_H	Fraction high affinity
F_L	Fraction low affinity
G protein	Guanine nucleotide binding protein
GABA	Gamma hydroxyl butyric acid
GDP	Guanosine diphosphate
GPCR	G protein coupled receptor
Gpp(NH)p	Guanosine 5'-[β,γ-imido]triphosphate
GTP	Guanosine tri-phosphate
IP_3	Inositol 1,4,5-trisphosphate
KCl	Potassium chloride
K_d	Dissociation equilibrium constant
LVEDP	Left ventricular enddiastolic pressure
LVSP	Left ventricular systolic pressure
mAChR	Muscarinic acetylcholine receptor
MAPK	Mitogen activated protein kinase
mRNA	Messenger RNA
NaCl	Sodium chloride
PCR	Polymerase chain reaction
PET	Positron emission tomography
PKA	cAMP dependent protein kinase
PMSF	Phenylmethanesulfonyl fluorid
PTX	Pertussis toxin
[^{3}H]QNB	1-quinacliinyl[phenyl-4^{3}H] benzilate
RV	Right ventricle
Sham	Sham operated
TME	Tris, magnesium chloride and EDTA

1 SUMMARY

The parasympathetic regulation of the heart may change in diseased states like congestive heart failure (CHF). In a functional study, a carbachol induced increased inotropic effect of muscarinic acetylcholine receptors (mAChRs) has been demonstrated in rats with CHF. The present study was undertaken to look for possible changes in mAChRs in CHF compared to normal cardiac ventricular membranes in rats.

Congestive heart failure was induced in male Wistar rats by coronary artery ligation. Corresponding Sham groups were prepared and served as control group. After 6 weeks, the ventricles from non-failing and failing hearts were isolated. In addition ventricles from normal, non-operated rats were isolated. Receptor binding experiments were performed in the corresponding myocardium.

No significant changes in the affinity of the radioligand, [^{3}H]QNB, for the mAChRs were observed in the ventricles from CHF rats compared to Sham rats (K_d value of 0.15 ± 0.04 nmol/L in CHF rats and 0.18 ± 0.06 in Sham rats). A tendency of increase in the mAChR density in CHF rats compared to Sham rats was obtained, but the increase was not significant (B_{max} of 175 ± 18 fmol/mg protein in CHF rats and 139 ± 11 fmol/mg protein in Sham). mAChRs possessed high- and low affinity binding sites for the non-selective agonist, carbachol, in the absence of guanosine trisphosphate (GTP). There were no significant differences in the affinity between normal, Sham and CHF rats. In the presence of GTP, a shift in affinity to a higher concentration of agonist was observed in normal, Sham and to a lesser extent in CHF rats. This indicated a lower sensitivity to guanine nucleotides of mAChRs in CHF rats. The mAChR subtype profile was characterised by using the subtype selective antagonists nitrocaramiphen, AF-DX 116, 4-DAMP and tropicamide. No significant changes in affinity of the chosen antagonists were observed in CHF rats compared to control group, and the receptor binding profile corresponded best to M_2 mAChRs. However, other mAChR subtypes and changes in the mAChR profile in CHF rats may be present and can not be excluded because of the lack of highly selective antagonists for mAChR subtypes.

2 INTRODUCTION

Cardiac function is dynamically regulated by the autonomic nervous system, i.e. sympathetic which acts via the active molecules noradrenaline and adrenaline, and parasympathetic nervous system, which acts via acetylcholine. These active molecules, called neurohormones, are produced in the neuroendocrine system and mediate their effect by adrenaline and noradrenaline binding to adrenoceptors and acetylcholine binding to muscarinic acetylcholine receptors. The regulation can be influenced by physiological factors and diseased states like congestive heart failure, and the balance between normal control of the heart and deleterious dysregulation might be shifted. The aim of this thesis was to look for possible changes in the muscarinic acetylcholine receptors in congestive heart failure by receptor binding experiments.

2.1 Congestive heart failure

2.1.1 Classification and pathophysiology

Congestive heart failure (CHF) has many definitions. One commonly used is a progressive pathophysiological state in which an abnormality of cardiac function is responsible for the failure of the heart to pump enough blood required by the metabolising tissues at normal chamber volumes and pressures (Remme and Swedberg, 2002). Patients with congestive heart failure have often symptoms of volume overload, like retention of fluid (congestion) in different parts of the body, such as legs, liver and lungs that cause shortness of breath and lung sound on the examination. Other symptoms may be related to inadequate tissue perfusion such as impaired exercise tolerance, fatigue and renal dysfunction. These symptoms will not be present in asymptomatic left ventricle dysfunction/heart failure when initial compensatory mechanisms are able to modulate left ventricle function to maintain the functional capacity.

Currently, heart failure is defined by four stages A-D (Table 1) complementing the traditional New York Heart Association (NYHA) classification (Table 2) (Cowie *et al.*, 1999;Hunt *et al.*, 2001), to recognise the initial risks and the progression of this syndrome.

Table 1: Heart failure is currently identified by four stages A-D according to the American College of Cardiology/American Heart Association guidelines.

Stage A	High risk of developing heart failure. No apparent structural abnormality of the heart.
Stage B	Structural abnormality of the heart but never had symptoms of heart failure.
Stage C	Structural abnormality of the heart. Current or previous symptoms of heart failure.
Stage D	End stage symptoms of heart failure that are refractory to standard treatment.

Table 2: The NYHA classification of congestive heart failure

Class I (Mild)	No limitation of physical activity. Ordinary physical activity does not cause any symptoms like fatigue, palpitation or dyspnea (shortness of breath).
Class II (Mild)	Slight, mild limitation of activity. Comfortable at rest, but ordinary physical activity causes fatigue, palpitation or dyspnea.
Class III (Moderate)	Marked limitation of activity. Comfortable only at rest, and less than ordinary activity causes fatigue, palpitation or dyspnea.
Class IV (Severe)	Unable to carry out any physical activity without discomfort. Symptoms of cardiac insufficiency at rest.

Congestive heart failure is a growing problem in the western countries. Approximately 2% of the population suffer from heart failure (Cowie *et al.*, 1999) and the syndrome becomes more common with increasing age. It is estimated that approximately 10% of persons over 74 years have heart failure or have had heart failure for a short period as a consequence of other cardiac diseases (Madsen, 1994;Gullestad and Madsen, 2004). Approximately one third of the patients with congestive heart failure are hospitalized during one year (Gullestad and Madsen, 2004) and the treatment of congestive heart failure is associated with high costs for the society (Haldeman *et al.*, 1999). Severe heart failure is a syndrome with a prognosis worse than many cancers. Half of the patients with chronic heart failure die within four years, and severe heart failure (NYHA class IV) has a one-year mortality of almost 50% (Cleland *et al.*, 1999). The cause of death seems to be either development of a more severe heart failure or arrhythmias (Gullestad and Madsen, 2004).

In the MERIT-HF study 91% of the deaths were caused by cardiovascular events (Hjalmarson *et al.*, 1999). Despite growing understanding of the regulation of cardiac function, more needs to be known about the basal mechanisms to develop new potent therapeutic strategies to be able to improve the prognosis for heart failure patients.

There are several causes of congestive heart failure, and if possible, preventing or treating the primary defect such as hypertension, is desirable. CHF can be caused by for instance ischemic heart disease, hypertension, arrhythmias, valve abnormalities and pericardial diseases. To maintain arterial pressure and perfusion of vital organs, different compensatory mechanisms are initiated which are the same as those being activated to increase cardiac output in daily situations. The most important responses are the Frank-Starling mechanism, myocardial hypertrophy, ventricular dilation and activation of neurohumoral systems, like release of noradrenaline, activation of the renin-angiotensin-aldosterone system and release of atrial natriuretic peptide (ANP). These mechanisms, some of them also called remodelling, can initially be adaptive and keep the blood supply sufficient for a short period to adapt to new requirements. However, they will over time become maladaptive, for instance during continued activation of neurohormonal responses in diseased states and initiate an unphysiological growth process by growth of the cells in length (i.e eccentric hypertrophy) that is accompanied with increased mechanical stress, increased protein synthesis, altered expression of genes regulating contractility, expression of fatal gene products and loss of cardiomyocytes by apoptosis or necrosis as some important factors (figure 1).

Overactivation of the adrenergic drive may be a result of both increased release and decreased reuptake of neurotransmitter, resulting in a constant exposure of the heart to levels of noradrenaline that are probably toxic to the heart (Braunwald and Bristow, 2000). Other changes in the adrenergic system are further described in part 2.3.1 “Adrenoceptors”. In heart failure the level of circulating and tissue concentration of angiotensin II is elevated causing increased ventricular afterload, myocyte hypertrophy, apoptosis, interstitial fibrosis, cardiac and vascular remodelling and increased secretion of aldosterone (Braunwald and Bristow, 2000). Activation of natriuretic peptides, endothelin and vasopressin may also play a critical role in the pathological

remodelling and thereby in the pathogenesis and progression of CHF (figure 1).

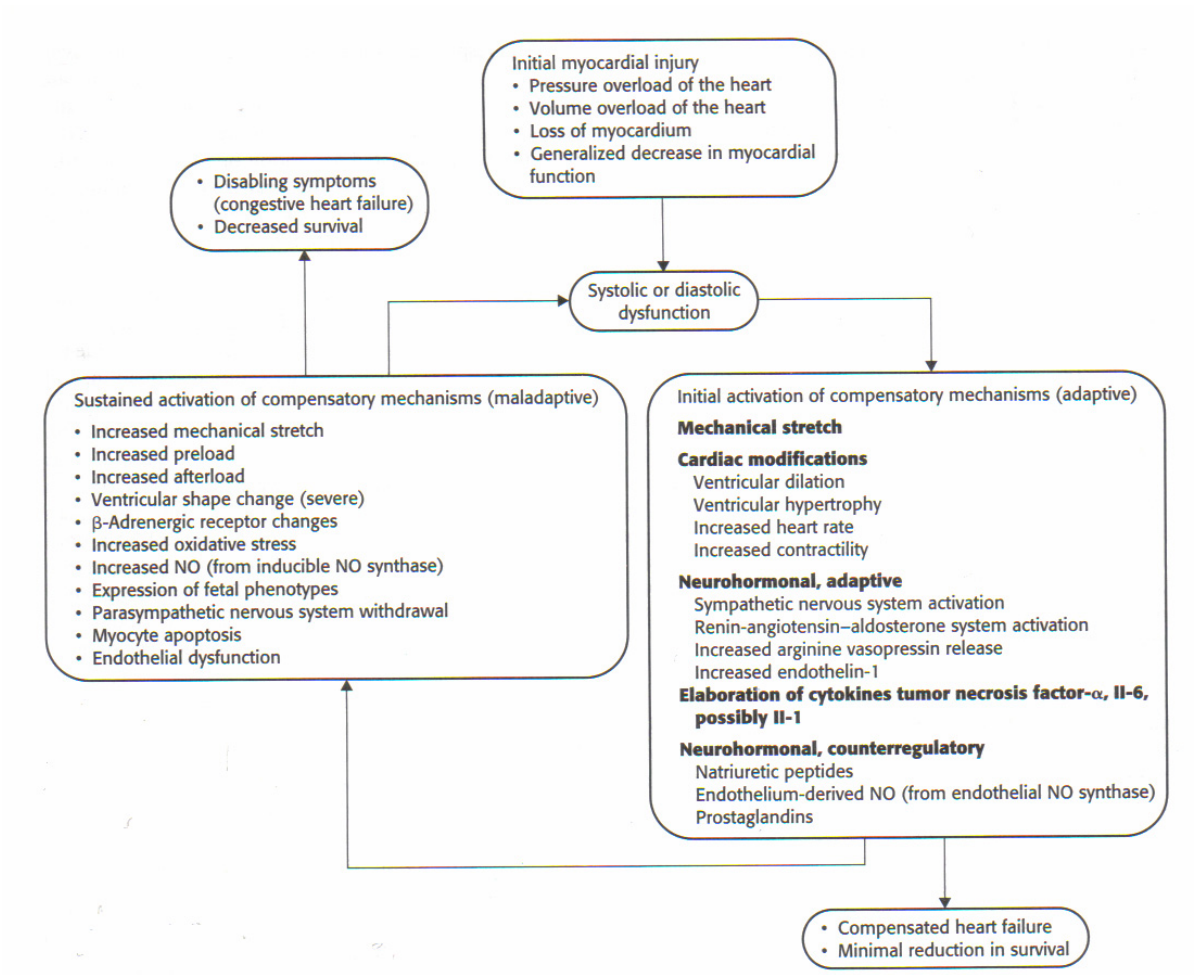

Figure 1: A schematic presentation of the pathogenesis of congestive heart failure. (After Textbook of Therapeutics: Drug and Disease Management (2000)).

2.1.2 Treatment of heart failure

The approaches to therapy are intended to treat the underlying causes, remove contributing factors that can worsen heart failure and treat the heart failure itself. When it comes to therapy, in the last few decades, there has been a change in the approach of therapy in heart failure. Until the 1980's, the attention was brought to altered hemodynamics as a cause of heart failure, and this model naturally directed the treatment. Positive inotropic drugs and vasodilators were the drugs of choice and the effect was characterised as changes in the hemodynamic factors. Since the 1980's the neurohormonal model is the main model because of the growing knowledge of the

importance of neuroendocrine systems in the development and the progression of heart failure. The drugs are designed to reduce the effect of the neurohormonal compensatory mechanisms that are initiated in heart failure. The treatment is currently based on β-blockers and ACE-inhibitors because of their beneficial effect on morbidity and mortality. The effect of β-blockers was not expected from a hemodynamic point of view because β-blockers reduce the inotropic effect. It was commonly thought that in heart failure it was necessary with increased adrenergic stimulation of the heart for adequate blood supply to the body.

Usually combinations of drugs with different targets are used for treatment of heart failure, depending on other additional diseases, underlying causes and types of CHF. Other examples of drugs used in drug therapy of heart failure are angiotensin II receptor antagonists, diuretics, aldosterone antagonists, heart glycosides, combined β- and α_1-AR antagonists and long acting nitrates.

2.2 G protein coupled receptors

2.2.1 Structure and classification of G protein coupled receptors

The most common type of receptors in the heart mediating the signals from neurohormonal stimulation is the guanine nucleotide binding protein (G protein) coupled receptors (GPCR). The most important examples in the heart are the adrenoceptors and the muscarinic acetylcholine receptors because they have an important function in the homeostatic regulation of the heart, but angiotensin, endothelin and the serotonergic receptors are also examples of GPCRs that participate in the homeostatic regulation. In addition several other kinds of receptors belong to the GPCRs, such as dopamine receptors, opiate receptors, purine receptors and receptors for many peptides (Rang *et al.*, 1999). A wide variety of physiological functions are regulated by GPCRs, and therefore, GPCRs are a major target for drug development. It was estimated in 2002 that 30% of the pharmaceutical drugs were ligands for GPCRs (Hopkins and Groom, 2002). Knowledge about the mechanisms of signalling of GPCRs is essential for understanding of the development of heart failure and further drug discovery.

GPCRs are divided in three main families according to their amino-acid sequence, where receptors from different families share essentially no sequence similarity (Bockaert and Pin, 1999). Family 1 contains most GPCRs and includes receptors for small ligands like catecholamines (1a), peptides (1b) and glycoprotein hormones (1c). Family 2 includes receptors for high molecular weight hormones such as glucagon. Family 3 contains receptors such as glutamate receptors, Ca^{2+} sensing receptor and gamma hydroxyl butyric acid-B ($GABA_B$) receptors, which have in common a very large extracellular domain. In addition, two other families have been described. Family 4 comprises pheromone receptors associated with G_i and family 5 includes receptors involved in embryonic development, cell polarity and segmentation. Finally cAMP receptors have been classified in one family since they have only been found in *D.discoideum.*

All GPCRs are cell surface receptors and have a common central core domain consisting of seven transmembrane α-helices connected by three intracellular and three extracellular loops. Most of the GPCRs also have two cysteine residues which form a disulfide bond. This may be important in packing and stabilising the conformations of the GPCRs. The intracellular carboxyl(C)-terminal domain, extracellular amino(N)-terminal domain and the intracellular loops differ in length and function which provide specific properties to the various receptor proteins (Bockaert and Pin, 1999).

GPCRs can recognise a diverse group of agonists, for instance light, Ca^{2+}, odorants, small molecules including amino-acid residues, nucleotides, peptides and proteins (Bockaert and Pin, 1999). The interaction between the agonist and the receptor may stabilise a change in the conformation of the core domain, generally in the second and third intracellular loop, constituting one of the key sites for G protein recognition and activation.

2.2.2 Heterotrimeric G proteins

G proteins are the signal mediators between the cell-surface receptor and the intracellular effectors. These proteins interact mostly with the third intracellular loop of the GPCRs. Activated G proteins mediate their function through enzymes and ion channels. Their interaction with the receptor may change in diseased states like heart failure.

G proteins are heterotrimeric and consist of α, β and γ subunits (Rang *et al.*, 1999). In the non-activated state, the α-subunit interacts with guanosine diphosphate (GDP) and is tightly associated with the βγ-complex. Upon activation of GPCRs by agonists, the α-subunit exchanges the bound GDP with GTP, resulting in the dissociation of the G protein from the GPCR and the dissociation of the α-subunit from the βγ-complex. The β- and the γ-subunits remain associated as a complex, anchored to the membrane through a fatty acid chain attached to an amino acid. The GTP-bound α-subunit and the βγ-complex can both regulate activities of different intracellular pathways, dependent on the class of G protein(s) activated (figure 2).

There is a variety of G proteins because of all the possible combinations of different subtypes of α-, β- and γ-subunits. At least 18 different subtypes of α-subunits have been identified (Wong, 2003). They can be divided into four subfamilies: 1) the G_s subfamily that stimulates adenylyl cyclase (AC), 2) the $G_{i/o}$ subfamily that inhibits AC and regulates ion channels, 3) the $G_{q/11}$ subfamily that activates phospholipase C β and 4) the $G_{12/13}$ subfamily where the knowledge is limited about its effects, but the $G_{12/13}$ subfamily seems to activate the Na^+/H^+ exchanger (Wong, 2003). Dependent on the subtype(s) of the G protein α-subunit that a GPCR interacts with, a single or a combination of effectors can be activated (Wong, 2003). A further description of the subfamilies is given in table 3 below. The great variety of G proteins which is also caused by the five subtypes of β-subunits and eleven subtypes of γ-subunits identified, gives the opportunity for a variety of combinations of G proteins and hence a diversity of activated intracellular pathways by GPCRs (Wong, 2003).

Table 3: Subfamilies of G proteins and examples of receptors, intracellular signalling and effects induced upon activation of GPCRs in the heart. AC, adenylyl cyclase; PLC-β, phospholipase C-β; IP_3, inositol 1,4,5-trisphosphate and DAG, diacylglycerol.

Example of receptors	**G proteins**	**Effectors**	**Second messengers**	**Effects**
β_1, β_2	G_s	AC Ion channels	↑cAMP Ion flux	Positive inotropic and chronotropic effect Increased metabolism
M_2, M_4	G_i	AC K^+ channel Ca^{2+} channel	↓ cAMP K^+ efflux	Negative inotropic and chronotropic effect
α_{1A}, α_{1B}, α_{1D} M_1, M_3, M_5	G_q	PLC-β	IP_3, DAG, Ca^{2+}	Positive inotropic effect
Unknown	$G_{12/13}$	e.g Na^+/Cl^- exchanger	e.g Na^+/Cl^- exchange	Limited knowledge about the distribution and the effects of $G_{12/13}$ in the heart
Several	βγ	e.g AC K^+ channels Receptor kinases	e.g ↓/↑ cAMP K^+ efflux	e.g Altered inotropy Receptor desensitisation

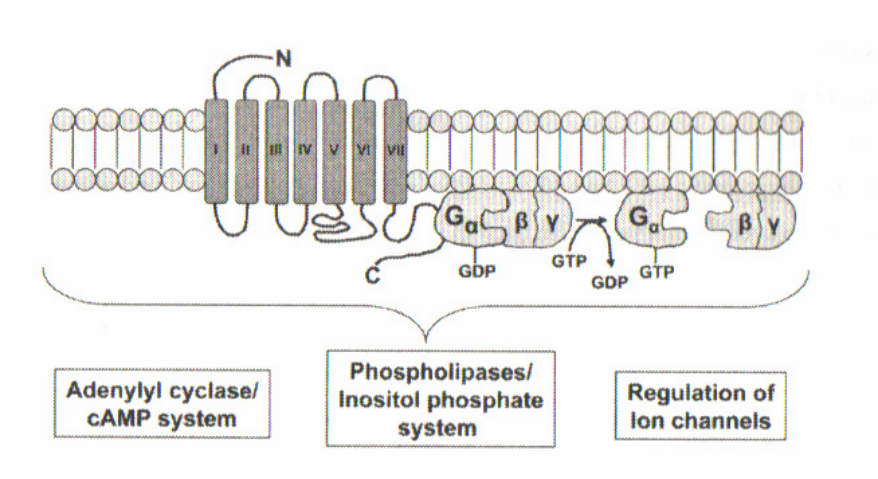

Figure 2: Seven transmembrane spanning (I-VII) G protein coupled receptor with an interacting G protein (α/βγ). Activation of the receptor catalyses the replacement of GDP with GTP on G_α, followed by dissociation of the G_α and $G_{\beta\gamma}$ subunits. Both subunits can interact with various proteins and initiate further signalling inside the cell. (After Qvigstad (2004)).

The activation of G proteins is terminated through the GTPase activity of the α-subunit, which hydrolyses GTP to GDP. This reaction causes the GDP bound α-subunit to reassociate with the βγ-complex, which allows several agonist-receptor complexes to activate several G proteins in turn and repetitive receptor-G protein coupling.

2.3 G protein coupled receptors involved in heart failure

The autonomic nervous system is important in the regulation of the heart and a further presentation of the functional receptors of the sympathetic and the parasympathetic nervous system is given below.

2.3.1 Adrenoceptors

Myocardial adrenoceptors belong to the family of G protein coupled receptors and are divided into three receptor types: α_1-, α_2- and β-adrenoceptors with further subtypes (figure 3). The endogenous agonists for these receptors are noradrenaline and dopamine released from sympathetic nerve endings and adrenaline released from the adrenal medulla.

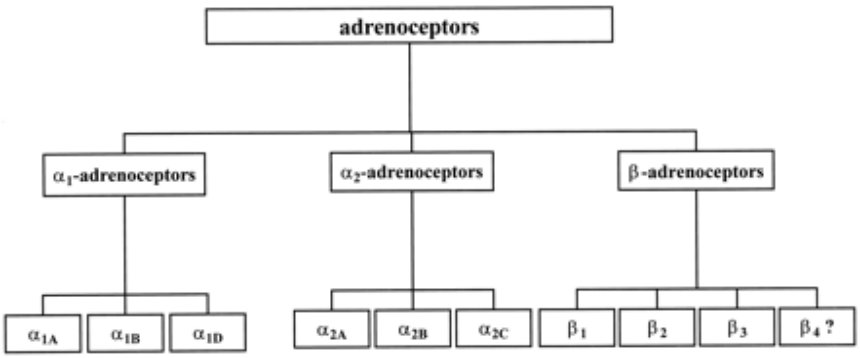

Figure 3: Adrenoceptor subtypes. (After Brodde & Michel (1999)). A putative β_4-AR has been discussed, but is now thought to represent a state of β_1-AR (Kaumann *et al.*, 2001).

Three subtypes of α_1-adrenoceptors (α_1-AR) have been identified through molecular cloning and pharmacologically (α_{1A}, α_{1B} and α_{1D}) (Brodde *et al*., 2001). In the rat heart all three subtypes have been identified at the mRNA level and α_{1B}-AR mRNA accounts for 50% of the total α_1-AR mRNA in the heart. Only α_{1A}-AR and α_{1B} –AR, however, seem to be expressed at the protein level in a ratio of 20% to 80% in rat ventricles (Michel *et al.*, 1994). α_2-adrenoceptors (α_2-ARs) are present in nerve terminals in the heart, but the presence of α_2-ARs postsynaptic on the cardiomyocytes is still a matter of debate.

α_1-ARs are assumed to couple primarily via a pertussis toxin (PTX)-insensitive G protein ($G_{q/11}$) to phospholipase C/inositol trisphosphate/diacylglycerol (PLC/IP_3/DAG) system (Brodde *et al.*, 2001). Activation of α_1-ARs mediates a slowly developing increased force of contraction (positive inotropic effect) which has been demonstrated in several species including human and rat, but the mechanisms involved are still a matter of debate. The increased IP_3-formation following α_1-AR stimulation, might mediate the release of Ca^{2+} from intracellular stores which could be involved. In addition, it has been found that α_1-AR stimulation increases the Ca^{2+}-sensitivity of myofilaments (Brodde *et al.*, 2001). Stimulation of α_1-ARs can also induce cardiac hypertrophy in rat, but it is unknown whether this phenomenon is present in the human heart (Brodde *et al.*, 2001). These effects suggest an important role in regulation of cardiac homeostasis, in rest, exercise and in diseased states. Little is known about the regulation of α_1-ARs in heart failure, but it has been speculated that α_1-ARs may function as a compensatory mechanism in the heart to maintain inotropy when the β-ARs are down regulated and uncoupled

(Sjaastad *et al.*, 2003). Because of the effects of α_1-AR stimulation and in agreement with the neurohormonal model, antagonism of α_1-AR may still have a beneficial effect in long term treatment of heart failure in combination with β-blockers, despite the observed higher incidence of stroke and combined cardiovascular disease in treatment with doxazosin, an α_1-AR antagonist, alone compared to treatment with diuretics (Davis *et al.*, 2000).

In the heart, three different β-adrenoceptor subtypes have been identified through cloning and pharmacologically and they are designed β_1, β_2 and β_3 (figure 3). The existence of a putative β_4-AR has been discussed (Brodde and Michel, 1999), but is now thought to represent a state of β_1-AR (Kaumann *et al.*, 2001). The β_1-AR is the predominant β-AR in mammalian heart and comprises about 70-80% of the total receptor number in normal ventricles.

Both β_1-ARs and β_2-ARs couple to G_s which stimulates AC and increases the cytosolic level of the second messenger cAMP. This in turn activates the cAMP dependent protein kinase A (PKA). PKA mediates phosphorylation of a variety of cellular effector proteins involved in the inotropic, lusitropic (cardiac relaxation), chronotropic (heart rate), growth promoting and cytotoxic effects. In addition, there is some evidence for β_2-AR coupling to G_i in mammalian species (Kilts *et al.*, 2000;Xiao *et al.*, 2004).

It is generally accepted that in patients with chronic heart failure, there is a decrease in cardiac β_1-AR both at the mRNA- and protein-level and an uncoupling of cardiac β_2-AR. There seems to be no change in the amount and functional activity of cardiac G_s, but an upregulation of the activity and amount of cardiac G_i (shown in most studies). Another change observed is an upregulation of mRNA levels and phosphorylation activity of cardiac β-AR kinase. There seems to be no change in the activity of the catalytic unit of adenylyl cyclase and PKA (Giessler *et al.*, 1999). Chronic stimulation of β-ARs has also seemed to induce expression of the cytokines tumour necrosis factor-α, interleukin-1 and interleukin-6 which may alter cardiac contraction, promote chamber enlargement, and thus play a significant role in the development of a dilated cardiomyopathy (Braunwald and Bristow, 2000).

2.3.2 Muscarinic acetylcholine receptors (mAChRs)

Muscarinic acetylcholine receptors mediate the parasympathetic control of the heart, and these receptors cause alternations in the inotropic and chronotropic response to catecholamines. Five different mAChRs have been cloned and identified pharmacologically so far, and they are designed M_1, M_2, M_3, M_4 and M_5 (Caulfield and Birdsall, 1998) (figure 4). The odd numbered subtypes of the mAChRs (M_1, M_3 and M_5) are coupled preferentially via $G_{q/11}$ to PLC and thereby formation of inositol phosphates, such as IP_3 and DAG. The even-numbered subtypes (M_2 and M_4) are coupled via G_i and hence to inhibition of adenylyl cyclase and thereby reduced intracellular cAMP (Caulfield and Birdsall, 1998).

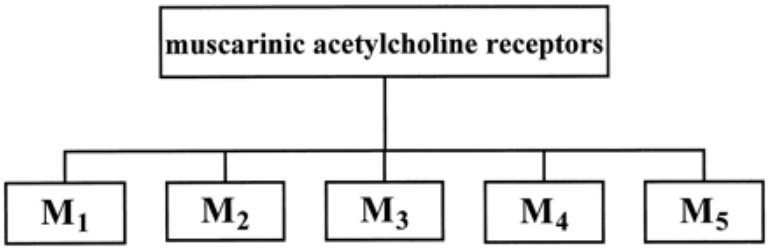

Figure 4: Muscarinic acetylcholine receptor subtypes. (After Brodde & Michel (1999)).

It is a general agreement that the main subtype of mAChRs in the heart of various mammalian species is M_2 mAChR (Brodde *et al.*, 2001;Dhein *et al.*, 2001). Stimulation of M_2 mAChRs causes negative inotropic and chronotropic effects in the heart. In atria, a direct negative chronotropic effect is mediated by stimulation of M_2 mAChRs and, in isolated tissue, inotropic effects. In the ventricles, however, the negative inotropic effect is only present when the basal force of contraction has been enhanced by cAMP-elevating agents, such as β-AR agonists, forskolin or phosphodiesterase inhibitors (Brodde and Michel, 1999). In addition to the common mechanism of inhibition of adenylyl cyclase, in atria acetylcholine opens potassium channels ($I_{K.Ach}$) by the G-protein βγ-subunit causing a reduction in the force of contraction.

Since M_2 mAChRs were long believed to be the only functional mAChRs in the heart, this tissue was commonly used as a model illustrating the exclusive presence of M_2 mAChRs. This concept

that the heart possesses only M_2 mAChRs has been challenged in the last decade. Many physiological responses to mAChR stimulation cannot be explained on the basis of a single M_2 mAChR subtype in the heart. Accumulating evidence suggests the existence of mAChR subtypes other than M_2 mAChR in cardiac tissues of chickens, rats, guinea pigs, rabbits, dogs and humans with large variations of subtype expression among species (Dhein *et al.*, 2001). Functional M_3 mAChRs in rat ventricular cardiomyocytes and human atria have recently been demonstrated (Willmy-Matthes *et al.*, 2003;Ponicke *et al.*, 2003). The presence of M_1 mAChRs was also demonstrated by RT-PCR detection both in guinea-pig and rat (Gallo *et al.*, 1993;Sharma *et al.*, 1997) and functional identification in rat (Sharma *et al.*, 1996). Quantification of the different mAChR subtypes at mRNA level by quantitative polymerase chain reaction (PCR) in normal rat heart showed that the M_2 mAChR mRNA represented more than 90% of total mAChR mRNA, while the concentrations of M_1, M_3, M_4 and M_5 mAChRs mRNA were less than 1%, 3%, 1% and 5% respectively (Krejci and Tucek, 2002).

There seem to be regional differences in the distribution of mAChRs in the heart. The parasympathetic innervation is denser in the sinoatrial and the atrioventricular nodes than in the left ventricle of the human heart (Kent *et al.*, 1974;Loffelholz and Pappano, 1985). The number of M_2 mAChRs is up to 2.5-fold higher in the atria compared to the ventricles (Brodde *et al.*, 2001). The distribution and functional responsiveness to M_2 mAChRs have in general been reported not to be altered in chronic heart failure (Brodde *et al.*, 2001;Dhein *et al.*, 2001). Less is known about the other mAChRs in CHF. However, Tveit found an increase in ventricular M_3 mAChR and M_4 mAChR at mRNA level in CHF rats compared to Sham rats (Tveit, 2003).

2.4 Background for the present study

Unpublished data from Hussain *et al*. showed a novel effect of mAChR stimulation in papillary muscles from rats with CHF. The same animal model of CHF was used as described in part 3.1.1 "Induction of myocardial infarction" in this thesis. Stimulation of papillary muscles with a β-AR agonist, isoproterenol, causes a positive inotropic response. This is a G_s mediated response through stimulation of AC and increase of cAMP resulting in an increase in the force of contraction. When this response was antagonised by a non-selective mAChR agonist, carbachol

(CCh), CCh did not only inhibit the β-AR stimulated inotropic effect, but it also elicited a positive inotropic response itself in the papillary muscles derived from rats with CHF (Hussain *et al*. unpublished). This inotropic response to CCh was more than 60% of the inotropic response mediated by the β-agonist, isoproterenol, in rats with CHF. This phenomenon seemed to be absent in papillary muscles derived from rats that had infarctions and no increase in left ventricular enddiastolic pressure (LVEDP) (Hussain *et al*. unpublished). This result may indicate that the response observed is a phenomenon in rats with CHF related to an increase in the LVEDP and not to the induced infarction and necrosis. To determine which mAChR subtype which mediates this CCh induced inotropic response, different selective antagonists for the different mAChR subtypes were used to try to antagonise this effect in dose-response curves. The chosen antagonists were nitrocaramiphen, an M_1 mAChR selective antagonist, AF-DX 116, an M_2 mAChR selective antagonist and 4-DAMP, an M_3 mAChR selective antagonist (see part 3.2.1 "Ligands and experimental conditions for the receptor binding assay" for more information on the selective antagonists). Only the selective antagonist for M_2 mAChRs, AF-DX 116, made a significant shift in the dose-response curve to a higher concentration of agonist which indicated that the CCh induced inotropic response was most likely mediated through M_2 mAChRs. This is in contrast to the well accepted hypothesis that M_2 mAChRs couple to G_i protein in normal heart, inhibiting AC and the formation of cAMP.

One of the hypotheses concerning the CCh induced positive inotropic response in the functional study described above is that the response is due to pathophysiological changes that occur in CHF. One suggestion is that the M_2 mAChRs may be coupled to two different pathways in CHF, one G_i protein mediated pathway by inhibiting AC and the formation of cAMP as described above one G_q protein mediated pathway by activating PLC which catalyses the formation of IP_3 and DAG. This could be present in the M_2 mAChRs as a change in affinity in CHF compared to normal hearts. However, other pathways cannot be excluded. One reason to suggest that M_2 mAChRs may be coupled to G_q protein is that the contraction-relaxation cycle of the CCh induced positive inotropic response resembles the contraction-relaxation cycle derived from α_1-AR- and endothelin-stimulated papillary muscles. Both the α_1-ARs and the endothelin receptors are G_q coupled receptors.

2.5 Aims of the present study

The aim of this study was to look for possible changes in muscarinic acetylcholine receptors in CHF compared to normal cardiac ventricular membranes by receptor binding experiments, using 6-week post myocardial infarction CHF rats as a model system.

More specifically it was of interest to:

1. Characterise the density of muscarinic acetylcholine receptors and their affinity for the radioligand used, [^{3}H]QNB, in cardiac ventricular membranes from CHF, sham operated and normal rats.

2. Study the interaction between muscarinic acetylcholine receptors and G proteins by examining agonist high-affinity binding and its regulation by guanine nucleotides in CHF, sham operated and normal rats.

3. Characterise the profile of muscarinic acetylcholine receptor subtypes in cardiac ventricular membranes from CHF, sham operated and normal rats by studying the binding affinity profile of several selective antagonists for the different mAChR subtypes.

3 METHODS

A general presentation of the methods is given in this chapter (part 3 “Methods”) while the details for the practical approach of this study, is presented in the protocols in the appendix (part 8.2 “Protocols”).

3.1 Heart tissue – the CHF model

3.1.1 Induction of myocardial infarction

Animals were cared for according to the Norwegian Animal Welfare Act and two rats were kept in each cage and housed in a temperature regulated room on a 12:12-h day/night cycle. The animals were given access to food and water *ad libitum*. An extensive infarction was induced by proximal ligation of the left coronary artery in approximately 200 g male Wistar rats under anaesthesia (68% N_2O, 29% O_2 and 2-3% isofluran (Abbot Park, Illinois, USA)).

Six weeks post infarction the rats were anaesthetised and ventilated as described above and catheterised for LVEDP measurements. CHF rats with a LVEDP $\geq$ 15 mmHg and a significantly increased heart and lung weight were included in the study (Sjaastad *et al.*, 2003).

Sham rats were operated in parallel and left ventricles from these rats were used as a control group in this study. They went through the same surgical procedure (a thoracotomy), but the coronary artery was not ligated.

Left ventricles from operated rats were all obtained from Institute for Experimental Medical Research, Ullevål University Hospital (Research group of professor Ole M. Sejersted).

3.1.2 Tissue sampling

During anaesthesia, the chest was opened in the rats and the heart removed. The ventricular tissue, separated in left and right ventricles, was immediately frozen in liquid nitrogen and kept frozen at –70 °C.

The normal rats, non-operated, obtained from Centre for Comparative Medicine, Rikshospitalet University Hospital, were anaesthetised with ether and killed. The chest was opened and the heart removed. The heart was perfused with 0.9% sodium chloride (NaCl). The heart atria were removed. The ventricles were immediately frozen by using the freeze-clamp method and the remaining atria tissue was removed with forceps. The heart tissue was kept frozen at -70 °C until smashing.

The heart was powdered in a mortar cooled in liquid nitrogen. The cardiac ventricular tissue was stored at – 70 °C until use.

3.1.3 Preparation of cardiac ventricular membranes

The membrane preparation was made as previously described by others (Mügge *et al.*, 1985) with modifications. The cardiac ventricular membranes had to be disrupted to increase access of the radioligand to the receptor population. During the tissue homogenisation, high levels of proteases can become available for receptor degradation. To prevent activation of proteolysis, denaturation of the receptors and loss of receptor binding sites, the tissue was kept frozen until it was used and kept cold during the whole preparation procedure by leaving all the equipment on ice while working. In addition cold solutions were used. Further addition of protease inhibitors may also be required to preserve the receptors. Ethylenedinitrilo tetraacetic acid (EDTA), a divalent cation chelating salt, was added to the tris, magnesium chloride and EDTA (TME) buffer in addition to phenylmethanesulfonyl fluorid (PMSF), an inhibitor of trypsin-like proteases and phenantroline, a metalloprotease inhibitor, which chelates iron, zinc and other divalent metals. PMSF and phenantroline were chosen according to other receptor binding studies in heart tissue performed by Jensen *et al*. and Dunlap *et al*.(1995;2003).

Myofilaments are present in the cardiac ventricular tissue. These large proteins can in receptor binding assays plug the glassfiber filters when filtration is the method of choice for separation of the receptor-radioligand complexes from unbound radioligand. To prevent plugging of the filters in this study, potassium chloride (KCl) at a final concentration of 0.5 mol/L was added initially to the homogenous membrane preparation. KCl was allowed to solubilise the myofilaments for 10 minutes while the membrane preparation was kept cold on ice before the washing of the membranes started.

Endogenous ligands for mAChR, such as acetylcholine, can interfere with the receptor binding. Therefore, it is necessary with a series of washing steps to remove the endogenous ligands. Especially for this study, it was important with several washing steps because of the competition experiments with carbachol in the absence and the presence of GTP. GTP is present in relatively high concentration in the heart tissue. If all the endogenous GTP had not been completely removed from the tissue during the washing procedure, this would have caused a shift in the calculated pK_i values from the displacement of [^{3}H]QNB by carbachol in the absence of added GTP.

Each membrane preparation was made from ventricular tissue from one heart. The membrane preparation was used fresh to avoid molecular changes by freezing.

3.2 Receptor binding assay

3.2.1 Ligands and experimental conditions for the receptor binding assay

The selected radioligand in this study was 1-quinacliinyl[phenyl-4^{3}H] benzilate ([^{3}H]QNB); specific activity 42 Ci/mmol, which is a non-selective antagonist for mAChRs that binds almost equally to all mAChR subtypes (Myslivecek and Trojan, 2003b) (figure 5). This compound has traditionally been used as ligand to label mAChRs at least from 1974 (Yamamura and Snyder, 1974). Because of the radioligand's physical-chemical properties, [^{3}H]QNB provides a simple, sensitive, specific assay for the mAChRs (Snyder *et al.*, 1975).

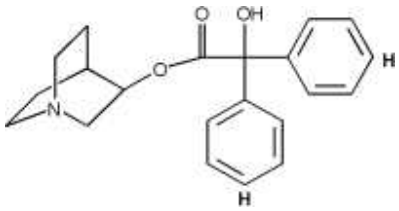

Figure 5: Structural formula: 1-quinacliinyl[phenyl-4^{3}H] benzilate, [^{3}H]QNB. The bold hydrogen atoms (**H**) represent the ^{3}H in the structural formula.

The binding experiments were performed by incubation of the cardiac ventricular membranes with the reagents for 120 minutes according to Myslivecek (2003a), except for the experiments to study if steady state was reached. However, the temperature was chosen to 24 °C to slow the reaction of proteases and to get an optimal receptor-G protein coupling, which is affected by a number of conditions and agents, such as pH, protein modification, proteases, ions and volatile anaesthetics (Aronstam and Narayanan, 1988). Aronstam and Narayanan also showed in 1988 that the guanine nucleotide sensitivity of agonist binding to mAChRs in rat atrium, was affected by the temperature. The guanine nucleotide effect was more expressed from 15 to 20°C (Aronstam and Narayanan, 1988). To avoid temperature variation, all the experiments were performed at 24° in a waterbath.

The incubation time must be sufficient for the interaction between the receptor and the radioligand to reach equilibrium as described in part 3.4.1 “Fundamentals of radioligand binding assay” and 3.4.2 “Saturation binding experiments”. To make sure equilibrium was obtained, saturation binding experiments with three critical concentrations of [^{3}H]QNB were incubated for 90, 120 and 150 minutes. Ventricular membranes from normal, Sham and CHF rats were used.

In all the binding experiments, the total binding was referred to as the amount of radioligand bound in the absence of a competing ligand for mAChRs. The binding in the presence of the competing ligand is referred to as non-specific binding, and the difference between the two is referred to as specific binding. In this study atropine, a non-selective antagonist, was used as competing ligand at a final concentration of 1 µmol/L as also previously published by others for instance Oki *et al*. (2001). Another unlabelled ligand than QNB itself was used to define the

specific binding to reduce the probability of including binding sites other than the mAChRs in the specific binding.

In addition to changes in receptor density and affinity studied in saturation binding experiments, changes in postreceptor mechanisms such as coupling to G proteins may underlie functional alterations in mAChRs transmission in CHF. This can be studied by examining agonist high-affinity binding and its regulation by guanine nucleotides. In this study, displacement of the chosen radioligand by carbachol, a non-selective agonist of mAChRs, was performed in the absence and the presence of GTP (for structural formulas see figure 6). The concentration of GTP used in the study was 100 µmol/L. Some additional displacement experiments were also performed with the non-hydrolysable analogue of GTP, guanosine 5'-[β,γ-imido]triphosphate (Gpp(NH)p) in the same concentration as GTP.

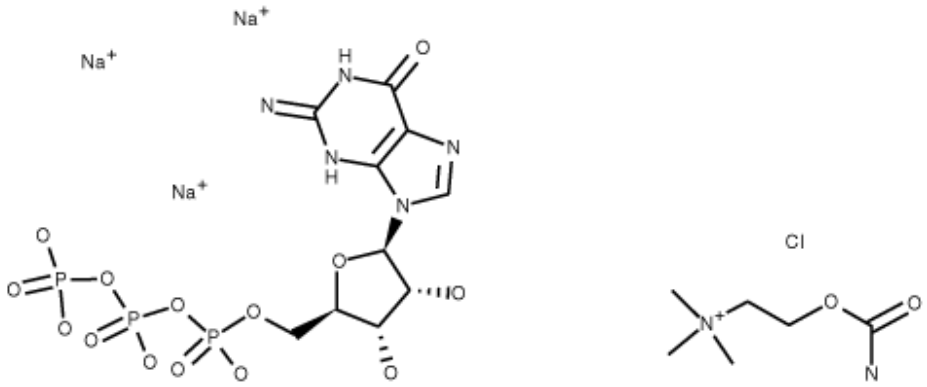

Figure 6: Structural formula: Guanosine 5'-triphosphate sodium salt (GTP) and carbachol

Development of selective antagonists for the mAChR subtypes has made it possible to pharmacologically discriminate between different mAChRs and characterise the receptor subtype profile. Several compounds are available, which show reasonable selectivity towards different mAChR subtypes. The selective antagonists in this study were the same as in the functional study for M_1, M_2 and M_3 mAChRs (Hussain *et al*. unpublished) and no second choice was done. In addition tropicamide was chosen as antagonist for M_4 mAChRs according to the published data for its affinity to M_4 mAChRs (table 4).

The antagonist for M_1 mAChRs used in this study was 2-Diethylaminoethyl 1-(4-nitrophenyl)cyclopentanecarboxylate hydrochloride, nitrocaramiphen (figure 7).

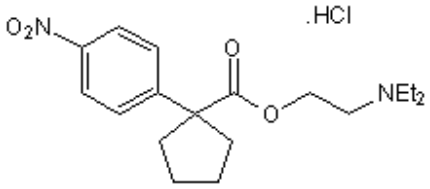

Figure 7: Structural formula: Nitrocaramiphen

The antagonist for M_2 mAChRs used in this study was 11-[[2-[(Diethylamino)methyl]-1-piperidinyl]acetyl]-5,11-dihydro-6*H*-pyrido[2,3-b][1,4]benzodiazepin-6-one, with the abbreviation AF-DX 116 (figure 8).

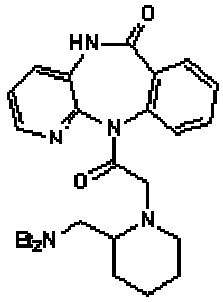

Figure 8: Structural formula: AF-DX 116

The selective antagonist chosen for M_3 mAChRs was 1,1-Dimethyl-4-diphenylacetoxypiperidinium iodide, with abbreviation 4-DAMP (figure 9).

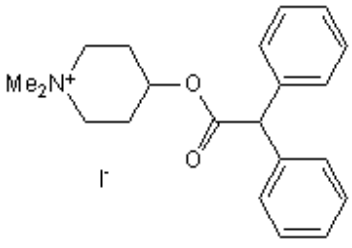

Figure 9: Structural formula: 4-DAMP

An antagonist with high affinity for M_4 mAChRs was *N*-Ethyl-3-hydroxy-2-phenyl-*N*-(pyridinylmethyl)propanamide, with abbreviation tropicamide (figure 10).

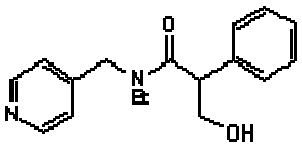

Figure 10: Structural formula: Tropicamide

There were no selective antagonists available with preferential affinity towards M_5 mAChRs (Wang *et al.*, 2004), and therefore, no affinity profile was obtained in this study for M_5 mAChRs.

Already published dissociation constants, K_i, for the selective antagonists used in the study and atropine are presented in table 4.

Table 4: Dissociation constants, K_i, for the selective antagonists (nitrocaramiphen, AF-DX 116, 4-DAMP and tropicamide) and atropine (Caulfield, 1993;Hudkins *et al.*, 1993;Eglen and Watson, 1996;Dhein *et al.*, 2001;Wang *et al.*, 2004). All the values are shown as pK_i (-log K_i). F, data from functional studies; C, data from studies on cloned receptors; B, data from radioligand-binding displacement studies.

	M_1 mAChR	**M_2 mAChR**	**M_3 mAChR**	**M_4 mAChR**	**M_5 mAChR**
Atropine	9.0-9.7	9.0-9.3	8.9-9.8	9.1-9.6	8.9-9.7
Nitrocaramiphen	B: 8.25	B: 6.4	B: 7.24	-	-
AF-DX 116	B/C: 6.4-6.7 F: 6.9	7.1-7.2	B: 5.9 F: 6.6	B/C: 6.6 F: 7	6.6
4-DAMP	8.9-9.2 C: 9.2	8-8.4 C: 8.4	8.9-9.3 C: 9.3	B/C: 8.9 F: 9.4	C: 9
Tropicamide	7.2	7.3	7.4	7.8	-

3.2.2 Separation of receptor-radioligand complex from the unbound radioligand – non-specific binding

The separation of the receptor-radioligand complex from the unbound radioligand, can be performed by both centrifugation and filtration. Filtration was chosen in this study because it is a more efficient method, requiring less handling of the samples. The termination of the reactions and the washing can be done much faster with filtration compared to centrifugation. Filtration is often the method of choice because the non-specific binding is usually lower. The high affinity of [^{3}H]QNB for the mAChRs (see part 4.2.2 "Binding properties of [^{3}H]QNB and muscarinic acetylcholine receptor density in rat ventricular membranes") combined with cold washing buffer will minimize the dissociation of the receptor-radioligand complex during the washing of the filters.

The radioligand, [^{3}H]QNB, may also interact with the glassfiber filters. This binding was not displaceable in the presence of 1 µmol/L atropine (data not shown). Because of this, the binding of [^{3}H]QNB to the filter was a part of the non-specific binding.

3.3 Protein quantification

To calculate the results from the study, it is commonly accepted to relate the amount of radioactive binding to the total amount of protein present. To determine the amount of protein in each sample, BC (bicinchoninic acid) Assay: Protein Quantitation Kit from Uptima and a Perkin Elmer HTS 7000 Bio Assay Reader was used. Proteins reduce Cu^{2+} in alkaline solutions to Cu^{+}. Two molecules bicinchoninic acid (BCA) react with each Cu^{+} resulting in a red water soluble complex with an absorption maximum of 562 nm. Absorbance is proportional to the total protein concentration between 5-20 µg/mL to 1-2 mg/mL, which allows spectrophotometric quantification of protein in aqueous solutions.

3.4 Receptor binding assays – analysis and calculations

3.4.1 Fundamentals of receptor binding assays

Receptor binding studies used to determine the affinity ($1/K_d$) of different substances for a given receptor and to determine the density of receptor in different tissues or samples are called saturation binding experiments. The method can also be used to measure the affinity ($1/K_i$) of unlabelled ligands for given receptors, called competition binding experiments. By using selective ligands, this method can be used to differentiate between receptor subtypes and characterise the receptor subtype profile.

The following criteria must be met to define a binding site a receptor and to be able to validate the binding assay (McKinney, 1998).

For binding sites to represent functional receptors, the binding needs to be specific which means it has to be displaceable by relevant unlabelled ligands in a relative low concentration range. All ligands, both agonists and antagonists, also have to inhibit the binding of the radioligand to the similar level of non-displaceable binding. The specific binding also needs to be characterised by the following criteria:

- The binding should be saturable, indicating a finite number of binding sites.
- The binding affinity, represented by the equilibrium dissociation constant (K_d), should be consistent with values determined for physiological receptors.
- The binding should be reversible, consistent with the physiological mechanism for dissociation of an endogenous ligand to a receptor.
- The binding site must have a relatively high affinity for the available ligands and a low or no affinity for other substances.
- The pharmacology of binding for both agonists and antagonists should be consistent with the pharmacology of the natural ligand in functional and whole-animal systems.

The binding of a radioactive ligand to a receptor is a bimolecular reaction according to the Law of Mass Action. A radioligand (L*) combines with a receptor (R) by diffusion and forms a complex (L*R) (McKinney, 1998):

$$L^* + R \underset{k_{-1}}{\overset{k_{+1}}{\leftrightarrow}} L^*R \qquad \text{Equation (1)}$$

The rate of the forward reaction is dependent on the concentration of L* and R and is given by the constant $k_{+1,}$ the association constant, which has the unit of ($time^{-1}$ x $concentration^{-1}$).

$$\text{Forward rate} = k_{+1} \times [L^*] \times [R] \qquad \text{Equation (2)}$$

The binding is reversible and the complex, L*R, starts to dissociate, dependent on the amount of the complex and the dissociation constant, k_{-1} which is expressed in units of $time^{-1}$.

$$\text{Reverse rate} = k_{-1} \times [L^*R] \qquad \text{Equation (3)}$$

At equilibrium, the rate of the association and the rate of the dissociation is equal and the amount of L*, R and L*R will be constant. The ratio of the rate constants (k_{-1}/k_{+1}) will be equal to the equilibrium dissociation constant, K_d.

$$K_d = \frac{k_{-1}}{k_{+1}} = \frac{[L^*] \times [R]}{[L^*R]} \qquad \text{Equation (4)}$$

K_d is expressed in units of concentration, such as nmol/L, and represents the concentration of ligand required to occupy 50% of the receptor in the tissue and is an expression for the affinity of the ligand for the receptor. According to the equations given above, one fundamental requirement in equilibrium binding experiments, such as saturation- and competition binding experiments, is that the reactants are incubated for sufficient time to reach equilibrium.

3.4.2 Saturation binding experiments

In a saturation binding experiment, increasing concentrations of the radioligand, [^{3}H]QNB, is incubated with the receptors, producing increasing concentrations of receptor-radioligand complexes. The theoretical maximal amount of receptor-radioligand complexes is called B_{max}, expressed as fmol/mg protein, and it represents the density of the mAChRs in the membrane preparation from the cardiac ventricles in this study. The results can be presented in a saturation plot, where the concentration of the radioligand bound to the receptor is presented as a hyperbola with the following equation:

$$[\text{Bound radioligand}] = \frac{B_{max} \times [\text{Free radioligand}]}{K_d + [\text{Free radioligand}]} \qquad \text{Equation (5)}$$

where the free concentration of the radioligand represents the concentration at the end of the incubation period. One practical criterion for this equation is that the receptor concentration has to be low enough for the free radioligand concentration at the end of the assay to be essentially equal to the concentration of ligand present at the beginning of the assay. If not, it is preferred to calculate the concentration of free radioligand at the end of the assay as the difference between the concentration of radioligand added and the concentration of radioligand bound, both non-specific and total.

The graphical method to precisely determine the K_d value and B_{max} is the Scatchard (Rosenthal) plot (Scatchard, 1949;Rosenthal, 1967). The concentration of bound/free (B/F) radioligand is plotted vs. bound (B) radioligand. A homogenous non-cooperative population of receptors will give a straight line, where the slope of the plot represents the negative of the inverse of the equilibrium dissociation constant, K_d and the x-intercept represents the theoretical maximal amount of specific binding sites, B_{max}. A non-linear Scatchard plot can be decomposed in two or more components, and may indicate multiple subtypes of receptors with different binding profile to the radioligand or cooperativities between receptors. A non-linear regression program in Microsoft Office Excel 2003 (by professor *dr.med* Finn Olav Levy, Department of Pharmacology, University of Oslo) was used to analyse the graphs as further described in part 3.4.4 “Calculations and statistics”.

3.4.3 Competition binding experiments

In a competition binding experiment, various concentrations of an unlabelled ligand compete with a fixed concentration of a radioligand, [^{3}H]QNB in this study, for binding to the receptor sites.

$$R + L^* + I \leftrightarrow RL^* + RI \qquad \text{Equation (6)}$$

where I presents the unlabelled ligand. The concentration of unlabelled ligand that inhibits 50% of the binding of the radioligand, [^{3}H]QNB, is called IC_{50}. The equilibrium dissociation constant for the unlabelled ligand for the receptor is called K_i. IC_{50} is related to both the ratio between the concentration of the radioligand, [L], and the K_d value, and the K_i value. Therefore, the K_i value can be obtained by using the Cheng-Prusoff equation (Cheng and Prusoff, 1973).

$$K_i = \frac{IC_{50}}{1 + ([L]/K_d)} \qquad \text{Equation (7)}$$

Analyses of the competition curves were performed by computer assisted program, GraphPad Prism® version 4 (GraphPad Software, CA, USA) assuming the existence of both low affinity sites and for high affinity sites. All experimental data were thus analysed for one or two binding sites by statistical evaluation.

3.4.4 Calculations and statistics

The affinity and density of muscarinic acetylcholine receptors were analysed and calculated by a non-linear regression program in Microsoft Office Excel 2003 with the Solver add in using the equation (5) (by professor Finn Olav Levy, Department of Pharmacology, University of Oslo). The non-specific binding was assumed to be linear and analysed by linear regression. The concentration of free [^{3}H]QNB was estimated as the difference between [^{3}H]QNB added and [^{3}H]QNB bound (non-specific and total). The specific binding data were fit to equation (5).

Scatchard plot as described in part 3.4.2 “Saturation binding experiments” was plotted for illustration. The displacement of [^{3}H]QNB by carbachol, atropine and the selective antagonists for the mAChR subtypes was analysed by using GraphPad Prism® version 4 (GraphPad Software, CA, USA) as described in part 3.4.3 “Competition binding experiments”. The curves were constructed as percent of maximum specific binding of the radioligand, [^{3}H]QNB, to the binding sites.

Data are expressed as mean ± standard error of the mean (S.E.M) and the number of animals are expressed as *n*. Statistical significance was estimated by Student’s t-test for comparing one- or two- binding site model with the statistical analysis in GraphPad Prism® version 4 (GraphPad Software, CA, USA). It was tested if a two-site model was significantly better than a one-site model. Significance level, α, was set to 0.05. A P value of ≤ 0.05 was considered statistically significant. Statistical analysis of the results was also performed by using Student’s t-test with the same statistical parameters. When appropriate, Bonferroni corrections were made in order to keep the level of significance.

A correlation test was performed between the different ΔpK_i values (all related to atropine) for the selective antagonists determined experimentally in this study and calculated from pK_i values published by others (presented in table 4). An estimated average of the published data for each antagonist was used in the test. A one-tailed Pearson correlation test was performed in GraphPad Prism® version 4 (GraphPad Software, CA, USA) since a positive correlation was estimated between the experimental data and the published data. R square values and P values were used to evaluate the correlation test.

4 RESULTS

This binding study is a part of the ongoing project with muscarinic acetylcholine receptors in congestive heart failure at the Department of Pharmacology, University of Oslo. This study is related to a functional study by Hussain *et al*. (unpublished).

4.1 Characteristics of Sham and CHF animals

The post infarction heart failure model in rats induced by coronary artery ligation showed hemodynamic changes characteristic for dilated cardiomyopathy with significantly increased heart weight including significantly increased right ventricle (RV) weight, elevated LVEDP ≥ 15 mmHg and decreased left ventricular systolic pressure (LVSP) which correspond to observed characteristics by others in this model (Sjaastad *et al.*, 2000;Sjaastad *et al.*, 2003;Tveit, 2003). Pulmonary congestion, an important sign of congestive heart failure, was also shown in the CHF rats by significantly increased lung weight. Animal characteristics are summarised in table 5.

Table 5: Animal characteristics. The values are given as mean ± S.E.M. RV, right ventricle; LVEDP, left ventricular end diastolic pressure; LVSP, left ventricular systolic pressure. * P < 0.05 ** P < 0.001
[#] Data obtained for only *n* = 7 in the Sham group, [##] Data obtained for only *n* = 23 in the CHF group

	Sham (*n* = 14)	**CHF (*n* = 24)**
Body weight, g	429 ± 13	386 ± 9*
Heart weight, g	1.46 ± 0.05	2.59 ± 0.11**
Heart weight/body weight, g/kg	3.43 ± 0.10	6.79 ± 0.30**
RV weight, g[#]	0.21 ± 0.01	0.44 ± 0.03**
Lung weight, g[##]	1.49 ± 0.04	4.01 ± 0.24**
LVEDP, mmHg[#]	7 ± 0.8	28 ± 1.6**
LVSP, mmHg[#]	130 ± 4	102 ± 3*

4.2 Binding characteristics of muscarinic acetylcholine receptors

4.2.1 Incubation time

For the results of the binding experiments to be valid, the experimental conditions have to be appropriate to allow the binding between the radioligand and the receptor to reach equilibrium for all the chosen concentrations of radioligand used in the assay. This is especially critical for the lowest concentrations, which require the longest time to reach equilibrium, according to equation (2) (part 3.4.1 "Fundamentals of receptor binding assays"). The incubation time was chosen to 120 minutes (Myslivecek *et al.*, 2003a). To confirm that the time chosen was appropriate under the given experimental conditions, specific binding was determined after 90, 120 and 150 minutes, for three low concentrations of the radioligand, [^{3}H]QNB (0.06 nmol/L, 0.22 nmol/L and 0.89 nmol/L) in ventricular membranes from normal, Sham and CHF rats.

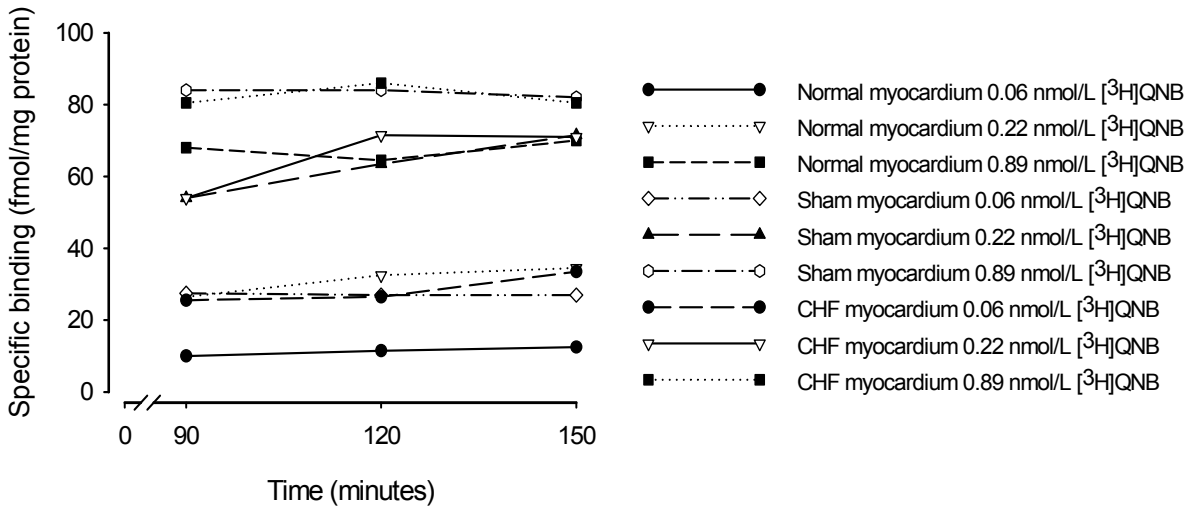

Figure 11: Time course of specific binding. Cardiac ventricular membranes from normal, Sham and CHF myocardium were incubated for 90, 120 and 150 minutes at 24 °C with 0.06 nmol/L, 0.22 nmol/L and 0.89 nmol/L [^{3}H]QNB. The figure shows the mean of two separate, similar experiments in each tissue.

As shown in figure 11, the specific binding of the [^{3}H]QNB for the mAChRs has reached a plateau at 120 minutes of incubation with the chosen concentrations of the radioligand. No further significant increase in specific binding was shown after 120 minutes. This indicated that

the incubation time chosen was long enough to reach equilibrium in the formation of receptor-radioligand complexes from mAChRs and free [^{3}H]QNB.

4.2.2 Binding properties of [^{3}H]QNB and muscarinic acetylcholine receptor density in rat ventricular membranes

It was of interest to determine the affinity of the radioligand, [^{3}H]QNB for the mAChRs and to determine the density of mAChRs in ventricular membranes from normal, sham operated and CHF rats and to compare the results from the different tissues to look for changes in the binding characteristics.

The specific binding of [^{3}H]QNB to muscarinic acetylcholine receptors in rat ventricular membranes displayed high affinity and was saturable as shown by a hyperbola given by equation (5) in figure 12. The non-specific binding, defined as non-displaceable binding in the presence of 1 µmol/L atropine, was non-saturable in the range of [^{3}H]QNB concentrations used. The non-specific binding was considered linear related to the [^{3}H]QNB concentrations.

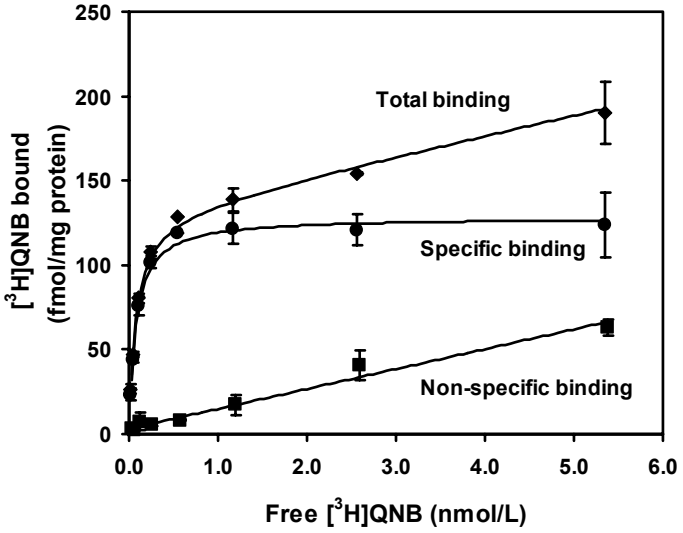

Figure 12: Saturation curve. The figure shows one representative saturation curve from one experiment in addition to the binding curve of the total binding and the non-specific binding of [^{3}H]QNB to binding sites in cardiac ventricular membranes from a CHF rat.

Scatchard plots of the data, one example showed in figure 13, gave a straight line, indicating a single population of receptors. This is in concert with the finding that the radioligand, [^{3}H]QNB, bound with equal affinity to the different mAChR subtypes (Myslivecek and Trojan, 2003b).

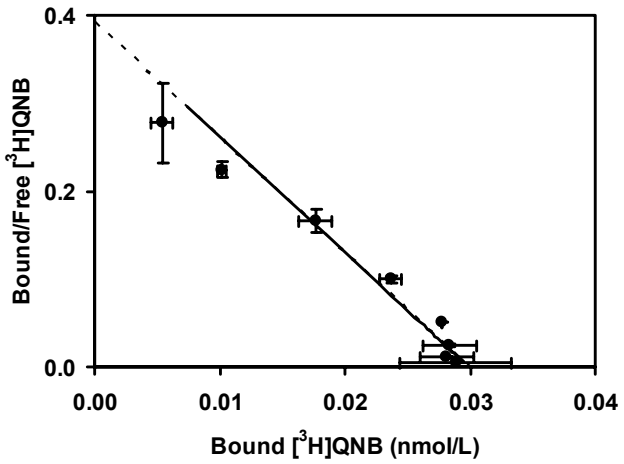

Figure 13: Scatchard plot. The figure shows the Scatchard plot for the same experiments as in figure 12.

There seems to be no significant change in the dissociation constant of [^{3}H]QNB for mAChRs in CHF rats compared to sham operated rats ($P > 0.05$) (table 6). B_{max} of mAChRs binding sites were increased by 26% in ventricular membranes from rats with CHF compared to sham operated rats, but this increase was not significant ($P = 0.085$) (table 6 and figure 14). There was, however, a significant increase by 29% in mAChR density between sham operated rats and normal rats ($P = 0.016$).

Table 6: Characteristics of muscarinic acetylcholine receptors in myocardium from normal, Sham and CHF rats measured by receptor binding.

Values are given as means ± SEM. K_d is given in nmol/L and B_{max} in fmol/mg protein.

	Normal (***n*** = 6)	**Sham** (***n*** = 6)	**CHF** (***n*** = 6)
K_d (nmol/L)	0.20 ± 0.02	0.18 ± 0.06	0.15 ± 0.04
B_{max} (fmol/mg protein)	108 ± 2	139 ± 11	175 ± 18

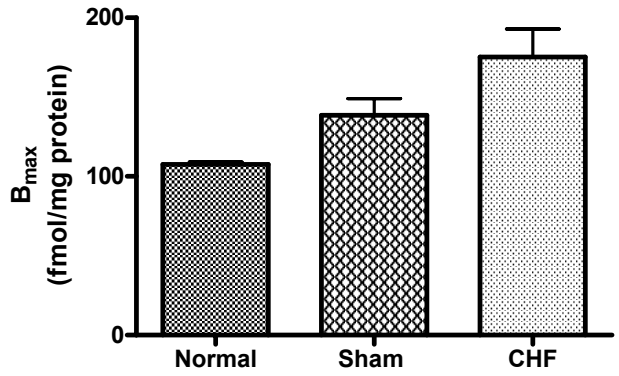

Figure 14: Muscarinic acetylcholine receptor density in normal, Sham and CHF rats. Values are given as B_{max} in fmol/mg protein.

4.2.3 Effects of guanine nucleotides on high-affinity agonist binding

Muscarinic acetylcholine receptor regulation of several cellular processes, including adenylyl cyclase activity, is mediated by G proteins. In this study, it was of interest to study the high-affinity binding of an agonist and its regulation by guanine nucleotides as an index of the interactions between the mAChRs and G proteins.

Carbachol was used as a non-selective agonist for the mAChRs and the [^{3}H]QNB binding was inhibited by carbachol in a dose-dependent manner (figure 15). The competition curve of carbachol was best fit to a two-site model in the absence of GTP in normal, Sham and CHF rats ($P < 0.05$), indicating the presence of both high- and low-affinity binding sites. There were no significant differences in the pK_i values for either high- and low-affinity binding sites or in the distribution between the two binding sites in normal, Sham and CHF rats ($P > 0.05$) (table 7).

In the presence of GTP added in excess, the G proteins get activated. GTP bound to the G proteins prevents the interaction with the receptor and hence make a shift of the carbachol competition curves to a higher agonist concentration (see figure 15 for examples and figure 16 for theoretical constructed competition curves based on the average data for fractions and pK_i values). The data did not fit significantly better to a two-site model than a one-site model for the

competition curves of carbachol in the presence of GTP ($P > 0.05$) in three of four experiments in ventricular membranes from normal rats, while a two-site model was preferred in four of eight experiments in Sham rats and in six of eight experiments in CHF rats ($P < 0.05$). There were no significant differences in the pK_i values between normal, Sham and CHF rats in the presence of GTP when all the binding experiments were presented as a one-site model (table 7).

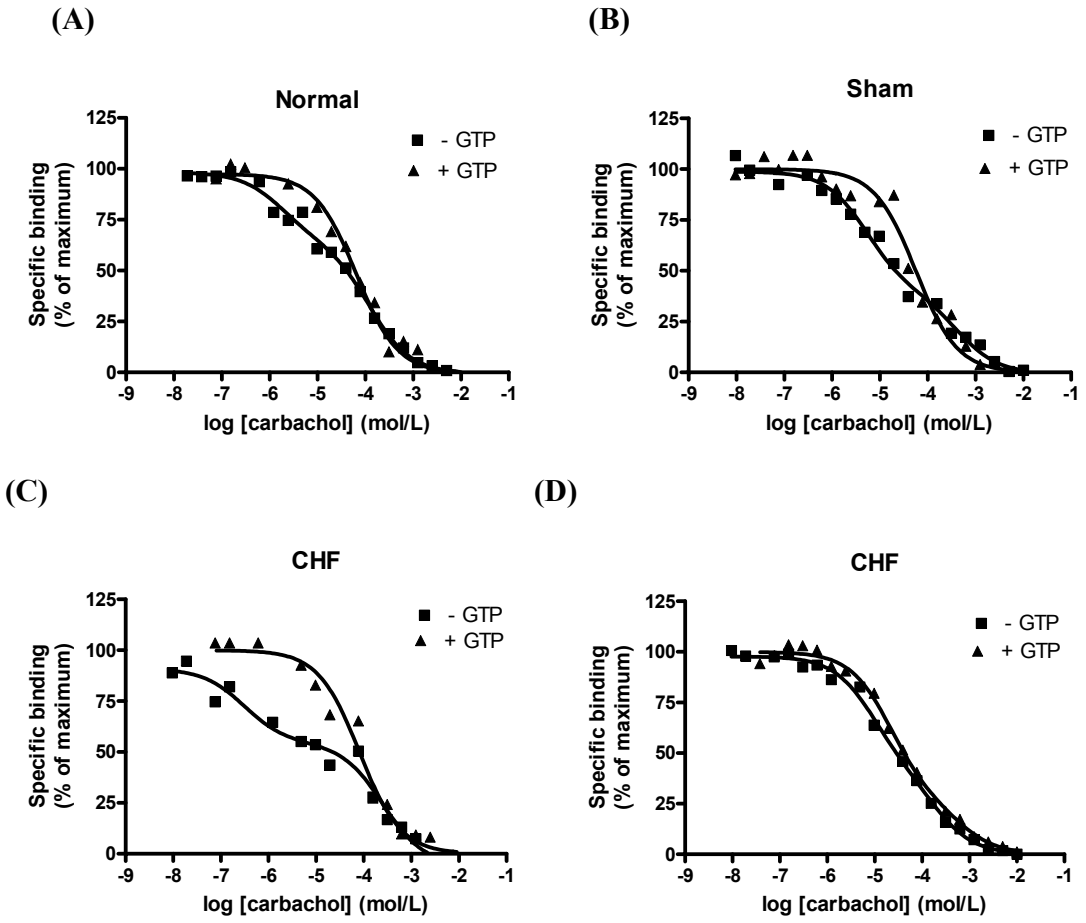

Figure 15: Dose-dependent competition by carbachol of [^{3}H]QNB binding to mAChR sites in ventricular membranes from normal rats (A), Sham rats (B) and CHF rats (C and D). Data are from single representative experiments. Panels **A**, **B** and **C** represent experiments where the carbachol competition curves were best fit to a two-site model in the absence of GTP and a one-site model in the presence of GTP. Panel **D** shows one of the experiments where a two-site model was preferred in the presence of GTP in ventricular membranes from CHF rats.

Table 7: Displacement of [^{3}H]QNB binding with carbachol to myocardial muscarinic acetylcholine receptors in normal rats, sham operated rats and rats with congestive heart failure. Values are given as means ± S.E.M. Affinity for the high affinity site (K_{iH}) and affinity for the low affinity site (K_{iL}) are given as pK_i (–log K_i). F_H, fraction high affinity; F_L, fraction low affinity. * Data in the presence of GTP in CHF rats analysed by a one-site model. ** Data in the presence of GTP in CHF rats analysed by a two-site model.

	Normal (***n*** **= 4)**	**Sham** (***n*** **= 8)**	**CHF** (***n*** **= 8)**	
In the absence of GTP:				
F_H	0.42 ± 0.06	0.45 ± 0.07	0.34 ± 0.07	
F_L	0.58 ± 0.06	0.55 ± 0.07	0.66 ± 0.07	
pK_{iH}	6.33 ± 0.21	6.42 ± 0.23	6.79 ± 0.29	
pK_{iL}	4.41 ± 0.11	4.52 ± 0.14	4.62 ± 0.15	
In the presence of 100 μmol/L GTP:			*	**
F_H	0	0	0	0.38 ± 0.09
F_L	1.00	1.00	1.00	0.62 ± 0.09
pK_{iH}	-	-	-	6.09 ± 0.17
pK_{iL}	4.88 ± 0.05	5.24 ± 0.11	5.20 ± 0.16	4.63 ± 0.13

From the data presented above, theoretical competition curves have been made based on the calculated averages of the fractions and the pK_i values for the high- and low affinity sites in the absence and the presence of GTP from normal, Sham and CHF rats. A two-site model for the competition curve of carbachol was chosen in the absence of GTP and a one-site model for the competition curve of carbachol in the presence of GTP (figure 16 A-C). However, in CHF rats, a two-site model was preferred in six of eight experiments in the presence of GTP. Therefore, it was decided to recalculate the data and make a theoretical competition curve based on the preferred two-site model in the presence of GTP for the CHF rats (table 7). The result is presented in figure 16 D.

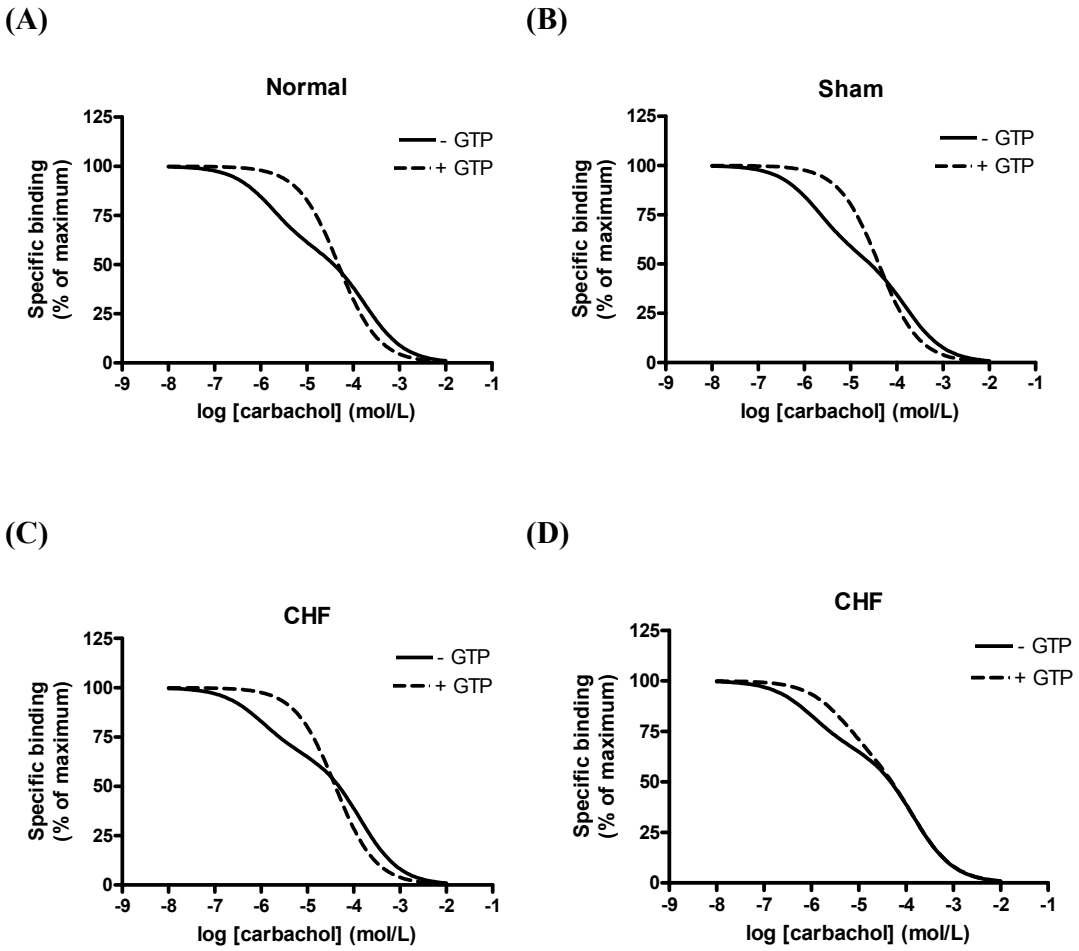

Figure 16: Theoretical calculated dose-dependent competition by carbachol of [^{3}H]QNB binding to mAChR binding sites in ventricular membranes from normal (A), Sham (B) and CHF rats (C and D). The curves are based on the calculated averages of the fractions and the pK_i values for the high- and the low affinity sites in the absence and the presence of GTP in ventricular membranes from normal, Sham and CHF rats. A two-site model was chosen for the competition curves in the absence of GTP, and a one-site model was chosen for the competition curves in the presence of GTP in **A**, **B** and **C**. However, in **D** a two-site model is presented for the competition curve in the presence of GTP in CHF rats.

Some additional experiments were performed in normal rats with carbachol in the absence and the presence of guanosine 5'-[β,γ-imido]triphosphate, Gpp(NH)p, a non-hydrolysable analog of GTP, and the results were similar to the already presented data, confirming that the GTP concentration chosen gave maximal effect (data not shown).

4.2.4 Muscarinic acetylcholine receptor subtypes in rat cardiac ventricles

To identify which mAChR subtypes are present in ventricular membranes in rats, different antagonists with high affinity for M_1 mAChRs (nitrocaramiphen), M_2 mAChRs (AF-DX 116) and M_3 mAChRs (4-DAMP) were used, chosen in accordance to the functional study (Hussain *et al*. unpublished). In addition, an antagonist for M_4 mAChRs (tropicamide) was used. Atropine was used as a reference substance for displacing mAChRs. Atropine inhibited the [^{3}H]QNB binding to mAChRs sites in a dose-dependent manner (figure 17). The competition curves were best fitted to a one-site model, and the pK_i values are presented in table 8. There were no significant changes in the pK_i values in congestive heart failure compared to the control group. A concentration of 1.0 μmol/L atropine displaced approximately 99% of the specific binding, and therefore this concentration of atropine was used to experimentally determine the non-specific, non-displaceable [^{3}H]QNB binding.

(A)

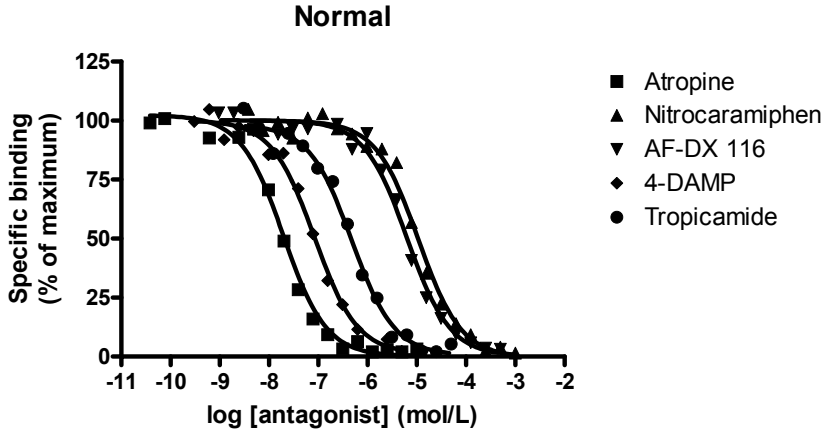

(B)

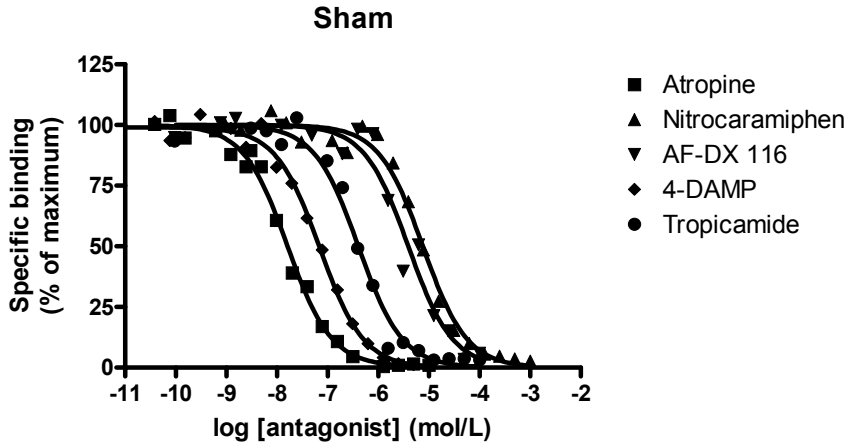

(C)

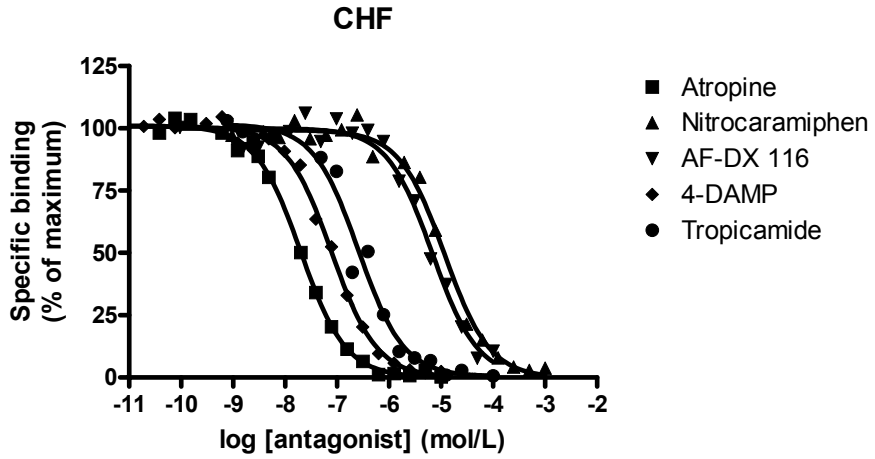

Figure 17: Competition curves. Inhibition of [^{3}H]QNB binding to mAChRs sites in cardiac ventricular membranes by atropine, nitrocaramiphen, AF-DX 116, 4-DAMP and tropicamide in normal (**A)**, sham operated (**B)** and CHF rats (**C**). The competition curves are from single, representative experiments.

Nitrocaramiphen, AF-DX 116, 4-DAMP and tropicamide all displaced [^{3}H]QNB binding in a dose-dependent manner. The competition curves for all the antagonists were best fitted to a one-site model for normal, Sham and CHF rats as shown in figure 17 ($P > 0.05$). The pK_i values are presented in table 8. There were no significant differences in the pK_i values comparing CHF to Sham and normal rats for any of the antagonists ($P > 0.05$).

Table 8: Competiton between [^{3}H]QNB and different antagonists for binding to myocardial muscarinic acetylcholine receptor sites in normal rats, sham operated rats and rats with congestive heart failure. Values are given as mean ± S.E.M. Ligand affinities are given as pK_i values (-log K_i).

	Normal	Sham	CHF
Atropine (*n* = 3)	8.45 ± 0.06	8.40 ± 0.06	8.45 ± 0.05
Nitrocaramiphen (*n* = 5)	5.67 ± 0.03	5.88 ± 0.06	6.04 ± 0.14
AF-DX 116 (*n* = 3)	5.93 ± 0.04	5.97 ± 0.13	6.12 ± 0.11
4-DAMP (*n* = 3)	7.79 ± 0.06	7.96 ± 0.09	7.99 ± 0.08
Tropicamide (*n* = 4)	7.05 ± 0.04	7.11 ± 0.08	7.25 ± 0.04

All the ligands used in the competition binding experiments, agonist (only carbachol in this study) and antagonists, displaced the radioligand, [^{3}H]QNB, to the similar non-specific, non-displaceable binding level. This common characteristic of all the ligands is an important indication that the radioligand binding sites represent the mAChRs present in the tissue.

5 DISCUSSION

Muscarinic acetylcholine receptors are important receptors in the dynamic regulation of the heart by the autonomic nervous system. This regulation may change during diseased states like congestive heart failure. Knowledge of the basal mechanisms is necessary to understand the pathophysiology of CHF, and it is important for further drug development.

5.1 Experimental considerations

Radioligand binding is a widely used pharmacological method to define and characterise the binding sites of interest that interact with a ligand that can be radiolabelled. In this study this method was used to examine characteristics of muscarinic acetylcholine receptors binding sites.

Many experimental conditions may influence the receptor-radioligand binding and the G protein interaction with the receptor, such as pH and temperature, and also contribute to changes in the receptor level, such as the presence of proteases in the tissue. Therefore, it is important to optimise the experimental conditions to obtain the correct determination of the receptor characteristics. How this process has been performed, can vary between different research groups and the results can be difficult to compare because the procedure for making the membrane preparation and other experimental conditions in the binding assay may be different.

In binding assays the radioligand will bind to all the available binding sites with affinity relevant for the actual concentration of radioligand. Therefore, the calculations of the density of the radioligand binding sites, the affinity of the radioligand and the pK_i values for the different agonists and antagonists to the receptors will represent the total amount of binding sites present in the tissue. In functional studies, a certain receptor mediated response is measured which is mediated by the signalling cascade downstream of one or several of the activated receptor subtypes present in the tissue and not necessary the whole receptor population which is available for the radioligand in binding studies. This may cause differences in the estimated pK_i values obtained from functional studies compared to receptor binding studies. This is important to bear

in mind when trying to explain a functional phenomenon, such as an inotropic effect mediated by CCh in CHF rats.

In receptor binding studies, the results represent the binding sites for the radioligand chosen. In this study, there is no measurement of functional response mediated by the same binding sites which could have confirmed that the binding sites represent muscarinic acetylcholine receptors except for the competition binding experiments with inhibition of [^{3}H]QNB binding by agonist in the absence and the presence of GTP. In these experiments, a conformational change in the binding site has been shown and this phenomenon is well-known for agonist binding to receptors. However, this study is strengthened by the finding that all the ligands used, both agonist and antagonists, displaced the radioligand binding to the similar level of non-specific, non-displaceable binding. All the ligands used displaced [^{3}H]QNB from the same pool of receptors, representing one or several mAChR subtypes.

5.2 Binding properties of [^{3}H]QNB and muscarinic acetylcholine receptor density in rat ventricular membranes

The affinity of the radioligand, [^{3}H]QNB, which is a non-selective antagonist for the mAChRs, was not significantly changed in ventricle membranes from rats with CHF compared to sham operated rats and normal rats. This fits well with already published data from heart in both rat and dog (Fu *et al.*, 1993;Dunlap *et al.*, 2003). The affinity of [^{3}H]QNB was also within the range of previously reported K_d values in heart from rats (Oki *et al.*, 2001;Dunlap *et al.*, 2003;Myslivecek and Trojan, 2003b).

In this infarction induced heart failure model in rats, the binding data may indicate an increase in mAChRs in ventricles from rats with CHF compared to Sham rats, but the alteration was not statistically significant. The same was observed in cardiac ventricular tissue from rat by Fu *et al*. (1993) even though the estimated density of mAChRs was generally higher in that study than found in the present work. This may be caused by different experimental conditions as described in part 5.1 “Experimental considerations”. In various other models of heart failure mAChR

density in ventricular myocardium has been reported to be reduced in a dog model of left ventricular failure due to aortic banding (Vatner *et al.*, 1988). Similar results were obtained in rats with aortic banding (Mertens *et al.*, 1995). In other studies of animal models with induced heart failure, the mAChR density has been showed to be increased (Vatner *et al.*, 1996). The receptor density in human cardiac tissue with heart failure has been shown to be unchanged in patients with end-stage heart failure due to idiopathic dilated cardiomyopathy or to ischemic cardiomyopathy while in the same patients β-AR numbers were significantly reduced (Böhm *et al.*, 1990a;Böhm *et al.*, 1990b). However, in an *in vivo* positron emission tomography (PET) study, cardiac mAChRs were shown to be slightly, but significantly increased in patients with congestive heart failure (Le Guludec *et al.*, 1997).

From the published data presented above, there seem to be variations in the results obtained in the different studies in the density of mAChR in heart failure compared to a control group. In some of the studies, the change in density of mAChR in heart failure seems to some extent to be related to the cause of heart failure. The tendency of increased mAChRs demonstrated in this study, in myocardium from rats with CHF due to myocardial infarction, might be some of the mechanism for the observed CCh induced positive inotropic effect in CHF rats (Hussain *et al*. unpublished).

5.3 Effects of guanine nucleotides on high-affinity agonist binding

Muscarinic acetylcholine receptors seem to be a population of receptors displaying both high and low affinity for agonists. The presence of guanine nucleotides promotes the conversion of receptors from a high-affinity to a low-affinity state (Rosenberger *et al.*, 1980). This leads to conformational states where receptors with high affinity for the agonist are coupled to G proteins, whereas receptors with low affinity for the agonist are uncoupled from the G protein (Aronstam and Narayanan, 1988). When comparing the fractions of receptors displaying high-affinity agonist binding in the absence of GTP between Sham and CHF rats, it is possible to provide information about receptor association with G proteins in congestive heart failure compared to the control group. The ability of guanine nucleotides to convert the receptors to low-affinity

states can also bring some information about the interaction between the receptors and the G proteins.

In this study there seemed to be no shift in the distribution between high- and low-affinity binding sites for carbachol in the absence of GTP in ventricular membranes from CHF rats compared to Sham and normal rats. The similar distribution between high and low affinity binding sites has also been reported in CHF rats and control group by Fu *et al*. (1993). The pK_i values for the high and low affinity in the absence of GTP were not significantly different in CHF rats compared to Sham and normal rats. This indicates that there is no change in the affinity for carbachol in CHF rats compared to Sham which was one of the hypotheses for the mechanisms of the carbachol induced inotropic effect in CHF rats (Hussain *et al*. unpublished).

In normal and Sham rats in the presence of GTP, a one site model was preferred in most of the experiments. This was expected according to the biological explanation of a shift in affinity for agonist in the presence of GTP since GTP bound to the G protein is expected to initiate the dissociation of the G protein from the receptor causing a conformational change of the receptor. When all the data were analysed by a one-site model in the presence of GTP, there were no significant changes in the low affinity between the different groups and there seemed to be no change in sensitivity to GTP. When comparing the low affinity pK_i values in the absence and the presence of GTP in normal, Sham and CHF rats, the pK_i values in the presence of GTP are nominally higher than in the absence of GTP. This may be caused by the mathematical calculations of a biological phenomenon including a small portion of high-affinity binding sites.

In the CHF rats, a one-site model of agonist binding in the presence of GTP did not seem to be the optimal presentation. In six of eight experiments in ventricular membranes from CHF rats, a two-site model was significantly better fitted to the data. When constructing competition curves based on the calculated averages of the fractions and the pK_i values using a two-site model both in the absence and the presence of GTP, the phenomenon of shift of the competition curves to a higher agonist concentration in the presence of GTP was still present, but to a lesser extent. A significant fraction of high-affinity binding sites was still present even if the pK_i value was

decreased. Thus, in the CHF rats, there may be a lower sensitivity to GTP. This finding was not further explored in this study, and the mechanism has to be further examined.

Since GTP can be hydrolyzed by GTPases present in the tissue, some additional experiments were done with Gpp(NH)p, a non-hydrolysable analogue of GTP, in normal rats. Since the results were not different from those shown with GTP, these experiments confirmed that the concentration of GTP used was sufficient to obtain maximal effect.

5.4 Muscarinic acetylcholine receptor subtypes in rat cardiac ventricles

Because of the indication of increased density of mAChRs in heart failure, it was of particular interest to identify which mAChR subtypes are present in ventricular membranes in normal, Sham and CHF rats. Altered expression of the mAChR subtypes may also be of interest since they mediate different effects: the M_2 and M_4 mAChRs are coupled to G_i, resulting in a negative inotropic and chronotropic effect; while the M_1, M_3 and M_5 mAChRs are G_q coupled and are expected to mediate a positive inotropic effect. Alterations in mAChR subtype expression may also be part of the explanation for the observed CCh induced positive inotropic effect in heart failure (Hussain *et al*. unpublished). Different selective antagonists for M_1, M_2, M_3 and M_4 mAChRs were used as tools to determine the receptor profile present in ventricles in normal, Sham and CHF rats, and if present, to detect changes in the receptor subtype profile in CHF rats compared to sham operated and normal rats.

Atropine was used as reference substance for displacement of [^{3}H]QNB since it is a commonly used non-selective antagonist for mAChRs. All the other ligands displaced the radioligand to the same level as atropine, indicating that the displaced radioligand represented the specific binding to mAChRs only even at high concentrations of the unlabelled ligands. The competition curve of atropine was analysed to best fit a one-site binding model, as expected. However, the calculated pK_i values of atropine from normal, Sham and CHF rats were approximately a half log unit lower

than the published data (table 4). This difference in affinity was taken into account when the receptor profile was analysed as described below.

The competition curves of the selective antagonists fitted a one-site binding model, which often indicate only one receptor subtype present in the tissue, or that the antagonists used in the study, are not able to distinguish between the different receptor subtypes. This is further discussed below.

The pK_i values for nitrocaramiphen in this study were calculated to 5.67 in normal, 5.88 in Sham and 6.04 in CHF rats, which was lower than the affinity published for nitrocaramiphen to M_1 mAChRs (table 4) and the affinity obtained in the functional study performed by Hussain *et al*. (unpublished) which was 7.57 in CHF rats. The pK_i values from the binding assays do not support the presence of M_1 mAChR in the ventricle in rats neither in CHF rats nor normal or Sham rats, but the measured affinities of nitrocaramiphen may fit to some extent with the affinity published for M_2 mAChRs for nitrocaramiphen (table 4). The M_2 mAChR antagonist, AF-DX 116, displaced [^{3}H]QNB with a low affinity compared to published affinity values for M_2 mAChRs (table 4). This was somewhat surprising, since one would expect to detect M_2 mAChRs to some degree since there has been a common agreement of this mAChR subtype as the dominant subtype present in the heart. The pK_i values were in this study calculated to 5.93 in normal rats, 5.97 in Sham rats and 6.12 in CHF rats. The affinities were also low compared to the pK_i values obtained in CHF rats in the functional experiments, 7.3 (Hussain *et al*. unpublished). The affinities of 4-DAMP to the mAChRs in this study were 7.79 in normal rats, 7.96 in Sham rats and 7.99 in CHF rats, which were clearly lower than the published affinities for 4-DAMP. Thus, our data do not support the presence of M_3 mAChRs as the dominant mAChR subtype based on the affinity of this antagonist separately (table 4). The pK_i value from the functional experiments was 8.38 in CHF rats (Hussain *et al*. unpublished). However, the affinity of 4-DAMP can be compatible with the presence of M_2 mAChRs according to the published data (table 4). Tropicamide, which is the antagonist used with high affinity for M_4 mAChRs, showed affinities of 7.05 in normal rats, 7.11 in Sham rats and 7.25 in CHF rats in this study. The affinities do not strongly support the presence of M_4 mAChRs in the ventricles, but tropicamide has almost the similar affinity to the other mAChR subtypes. Therefore, it is not possible to

distinguish between the other mAChR subtypes by using tropicamide. Functional experiments with tropicamide were not performed when this thesis was written.

In general, based on the pK_i values calculated from this receptor binding study compared to the pK_i values obtained from the functional experiments (Hussain *et al*. unpublished), the data obtained seem to indicate that in receptor binding experiments the radioligand labels a different population of mAChRs than the mAChR subtypes mediating the observed positive inotropic effect by CCh in CHF rats. This can be explained as previously stated by only a fraction of the present mAChRs in the ventricular membranes mediating the observed effect and thus only the characteristics of those receptors are exposed in functional studies.

To identify the mAChRs present in the ventricles in rats, the result can not completely rely on evaluation of affinity of a single antagonist for one mAChR subtype. The whole profile of affinities of the different antagonists has to be considered. Therefore, a correlation test was done between the obtained pK_i values for all the selective antagonists in the receptor binding study and the published data for the antagonists in relation to identified mAChR subtypes. No published pK_i values for nitrocaramiphen to M_4 mAChRs and M_5 mAChRs and tropicamide to M_5 mAChRs were obtained from the published data. Because of this, a correlation test could only be made from the pK_i values obtained from the receptor binding experiments and the published data for M_1, M_2 and M_3 mAChRs. Since the pK_i values for atropine obtained in this study was lower than the published data (table 4), ΔpK_i values for all the selective antagonists were calculated relative to the pK_i value of atropine in normal, Sham and CHF rats. A Pearson correlation was performed and the results are presented in figure 18 A-I. The binding profile for the antagonists in normal, Sham and CHF rats seems to be best correlated with the M_2 mAChRs with r square values of 0.84, 0.82 and 0.80 and P values of 0.04, 0.05 and 0.05, respectively. This fits well with the theory that M_2 mAChRs are the dominant mAChR subtype expressed in the heart. The presence of M_3 mAChRs in the ventricles can not be completely excluded based on the result from the correlation test with r square values of 0.67, 0.74 and 0.73 and P values of 0.09, 0.07 and 0.07 in normal, Sham and CHF rats, respectively, but it does not seem to be the dominant mAChR subtype. As previously described, a functional role of M_3 mAChRs has been demonstrated in both rat and human heart (Ponicke *et al.*, 2003;Wang *et al.*, 2004). From the

correlation test, the probability of the presence of M_1 mAChRs seems to be low based on the obtained data. However, at the mRNA level, M_1 and M_3 mAChRs seem to constitute only a small fraction of the mAChRs in the heart, 1% and 3%, respectively (Krejci and Tucek, 2002). Studies performed by both Krejci & Tucek (2002) and Tveit *et al*. (2003) detected mRNA for all the mAChR subtypes in left ventricle in rat, indicating that M_2 mAChRs are not the only mAChRs in the heart, at least not at the mRNA level. If the same mAChR subtype profile is present at the protein level, it can be difficult to detect with receptor binding performed with the selectivity of the synthetic ligands available today. There exist no ligands with high affinity for M_5 mAChRs, and the already existing antagonists for the other mAChR subtypes seem to show varying extents of overlap in affinity between the different subtypes. The data obtained in this study seem to indicate that M_2 mAChRs are the main mAChR subtype in rat ventricles. Based on other functional and biochemical studies, there is probably a mixture of several mAChR subtypes, which may also be present in the tissue examined in this study. However, the tools currently available may not be adequate to determine this in binding studies.

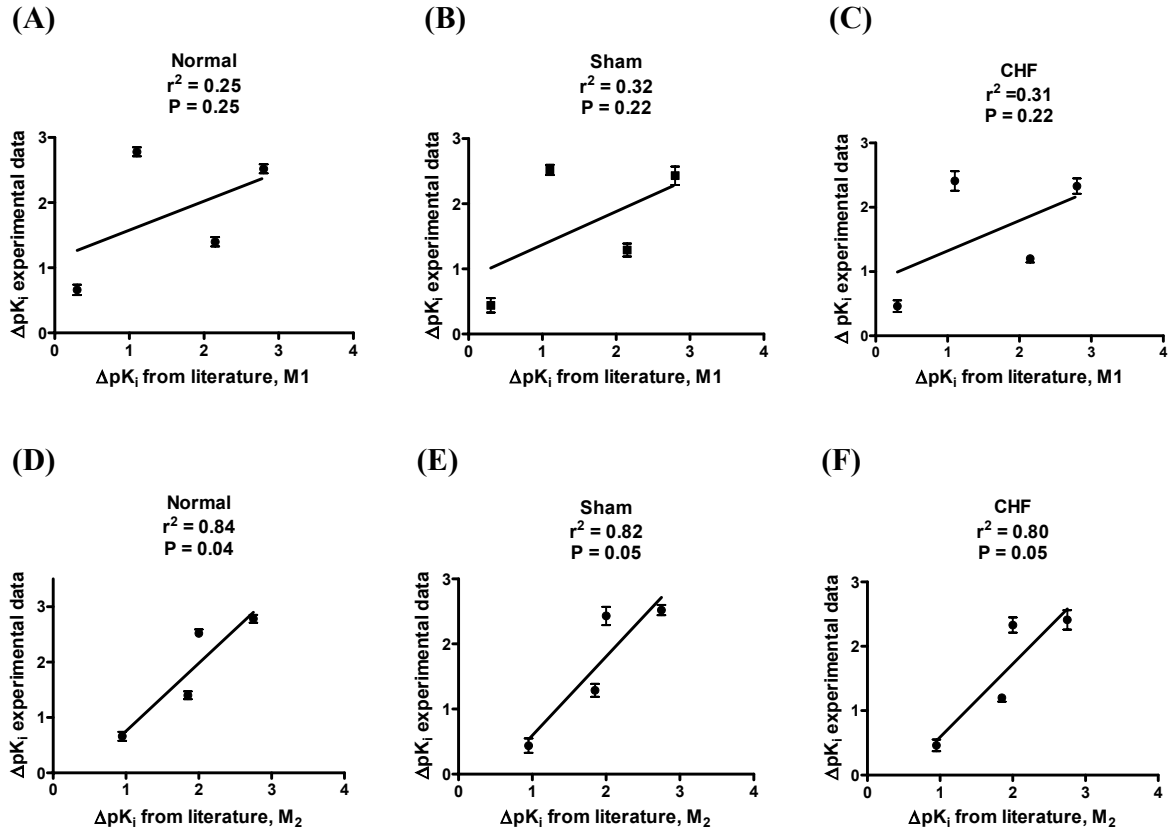

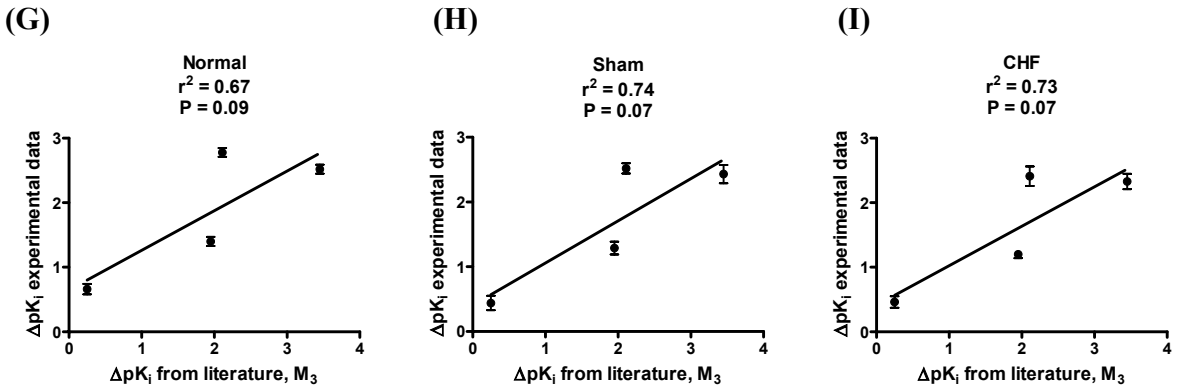

Figure 18: Correlation curves between ΔpK_i values obtained from the experimental data in this study and the ΔpK_i values from the published data (table 4) for M_1 mAChRs (A-C), M_2 mAChRs (D-F) and M_3 mAChRs, (G-I) in ventricular membranes from normal, Sham and CHF rats. Values are presented as ΔpK_i values (± S.E.M for the experimental data). A one-tailed Pearson correlation test was performed since a positive correlation was estimated.

The fact that the available selective antagonists for mAChR subtypes may not be selective enough to identify low levels of certain subtypes and hence detect small changes in receptor subtypes is important to bear in mind when evaluating and comparing the receptor subtype profile between CHF rats and normal and Sham rats. There were no significant differences in the pK_i values for any of the antagonists in CHF rats compared to normal and Sham rats ($P > 0.05$), which indicated no measurable changes in the mAChR profile in ventricular membranes from CHF rats compared to Sham and normal rats. This was also shown in the correlation test with very similar r square values from normal, Sham and CHF rats. The result from the study by Tveit *et al*. (2003) indicated that the M_2 mAChR mRNA level did not change in an infarction induced CHF model in rats, which was the same model as used in this study. Giessler *et al*. (1999) also claimed that cardiac M_2 mAChR density and functional responsiveness in failing human heart were not considerably changed. However, Tveit *et al*. (2003) showed an increase at the mRNA level of both M_3 mAChRs and M_4 mAChRs in CHF compared to Sham rats. This might indicate that these two subtypes of mAChRs may become more important in CHF in rats. The functional positive inotropic effect of CCh in papillary muscles from CHF rats observed in our lab (Hussain *et al*. unpublished) seemed to have characteristics indicating that the effect was mediated by a G_q coupled receptor, possibly implicating the M_3 mAChR. However, the increased level of M_3 and M_4 mAChR at the mRNA level does not necessarily result in increased receptor proteins. Even if

a change was present, the increased fraction may be too small to be detected in receptor binding studies with the selective antagonists available today.

By using pharmacological techniques like receptor binding assays, the result will rely on the identification of receptor profiles, compared with receptor binding profiles usually quantified for receptor ligands acting on a pure and homogeneous receptor population. This can be done by using transfected cell lines expressing one particular mAChR gene. However, caution has to be shown when using this comparison because an assumption that the cloned receptor expressed in the cell line will have the same characteristics as the native expressed receptor in the intact organism may be wrong. Caulfield suggested in his paper from 1993 that mAChR amino acid sequences have sites that are likely targets for post-translational modification, such as phosphorylation or glycocylation, and the native cell complement of moieties that can couple to the receptor, such as G protein, may result in differences in ligand-binding affinities between receptors expressed in transfected cells and in native cells. It should also be noted that several antagonists, such as gallamine, allosterically modulate mAChR function, notably at the M_2 mAChRs (Eglen and Watson, 1996;Christopoulos and Kenakin, 2002). This may complicate the determination of their apparent affinity and thus interpretation of subtype selectivity.

5.5 Future Research

For the understanding of pathophysiology of congestive heart failure, it would be of interest to examine the mechanism causing the decreased sensitivity of G proteins for guanine nucleotides in ventricles from rats with congestive heart failure. The first approach may be to determine which G protein is present in the ventricle and if there are changes in the G protein type or recruitment of other G proteins to the cell membranes in congestive heart failure compared to a control group.

To identify mAChR subtypes in ventricles in rats by a pharmacological method like receptor binding, there seems to be a need for new synthesised selective antagonists for the different mAChR subtypes with higher selectivity between the mAChR subtypes than the “selective”

antagonists available today. It may then be possible to detect the presence of even small amounts of subtypes and changes in receptor profiles if present in diseased states like congestive heart failure. It would also have been of interest to have radiolabelled selective antagonists which could make it possible to label the mAChRs subtypes and to do competition binding experiments with another unlabelled selective antagonist. Then the calculated pK_i values would make a more precise determination of the receptor profile. To be able to correlate the affinities of the antagonist with affinities for each mAChR subtypes, the affinity for each of the antagonists had to be determined separately for each mAChR subtype in a cell line with over expression of the different mAChR subtypes.

Until more satisfying selective antagonists have been developed, other biochemical methods may be used to identify the mAChR profile at receptor level in ventricles from rat, such as antibodies which recognise each mAChR subtype and can quantitatively determine the amount of each subtype present in the tissue.

6 CONCLUSION

In conclusion, it has been demonstrated that there might be no significant change in muscarinic acetylcholine receptor density in ventricles from rats with congestive heart failure induced by infarction compared to control group, even though a non-significant increase was observed. No change in affinity for the agonist carbachol seemed to be present in CHF rats compared to control group in the absence of guanine nucleotides. However, the mAChRs in the ventricles from CHF rats seemed to have lesser sensitivity to GTP than mAChRs in the ventricles from normal and Sham rats. The mechanism is still unknown. The dominant mAChRs in the ventricles in rat seemed to be M_2 mAChRs, and no change in mAChR subtype profile in the ventricles in CHF rats compared to control group was observed. However, the selective antagonists for the different mAChR subtypes, currently available today, might not be able to detect small fractions of mAChR subtypes even if they were present in the cardiac ventricular membranes, or to detect small differences in the expression of receptor proteins in congestive heart failure compared to control group.

7 REFERENCE LIST

(2000) *Textbook of Therapeutics : Drug and Disease Management*. Lippincott Williams Wilkins, Philadelphia.

Aronstam RS and Narayanan TK (1988) Temperature effect on the detection of muscarinic receptor-G protein interactions in ligand binding assays. *Biochem Pharmacol* 37: 1045-9.

Bockaert J and Pin JP (1999) Molecular tinkering of G protein-coupled receptors: An evolutionary success. *EMBO Journal* 18: 1723-9.

Böhm M, Gierschik P, Jakobs K-H, Pieske B, Schnabel P, Ungerer M and Erdmann E (1990a) Increase of $G_{i\alpha}$ in human hearts with dilated but no ischemic cardiomyopathy. *Circulation* 82: 1249-65.

Böhm M, Ungerer M and Erdmann E (1990b) Beta adrenoceptors and m-cholinoceptors in myocardium of hearts with coronary artery disease or idiopathic dilated cardiomyopathy removed at cardiac transplantation. *American Journal of Cardiology* 66: 880-2.

Braunwald E and Bristow MR (2000) Congestive heart failure: fifty years of progress. *Circulation 102(20 Suppl 4):IV14-23*.

Brodde O-E, Bruck H, Leineweber K and Seyfarth T (2001) Presence, distribution and physiological function of adrenergic and muscarinic receptor subtypes in the human heart. *Basic Research in Cardiology* 96: 528-38.

Brodde O-E and Michel MC (1999) Adrenergic and muscarinic receptors in the human heart. *Pharmacol Rev* 51: 651-89.

Caulfield MP (1993) Muscarinic Receptors--Characterization, coupling and function. *Pharmacology & Therapeutics* 58: 319-79.

Caulfield MP and Birdsall NJ (1998) International Union of Pharmacology. XVII. Classification of muscarinic acetylcholine receptors. *Pharmacol Rev* 50: 279-90.

Cheng Y and Prusoff WH (1973) Relationship between the inhibition constant (K_I) and the concentration of inhibitor which causes 50 per cent inhibition (I_{50}) of an enzymatic reaction. *Biochemical Pharmacology* 22: 3099-108.

Christopoulos A and Kenakin T (2002) G protein-coupled receptor allosterism and complexing. *Pharmacol Rev* 54: 323-74.

Cleland JGF, Gemmell I, Khand A and Boddy A (1999) Is the prognosis of heart failure improving? *European Journal of Heart Failure* 1: 229-41.

Cowie MR, Wood DA, Coats AJS, Thompson SG, Poole-Wilson PA, Suresh V and Sutton GC (1999) Incidence and aetiology of heart failure; a population-based study. *Eur Heart J* 20: 421-8.

Davis BR et al. (2000) Major cardiovascular events in hypertensive patients randomized to doxazosin vs chlorthalidone: The antihypertensive and lipid-lowering treatment to prevent heart attack trial (ALLHAT). *Journal of the American Medical Association* 283: 1967-75.

Dhein S, van Koppen CJ and Brodde OE (2001) Muscarinic receptors in the mammalian heart. *Pharmacol Res* 44: 161-82.

Dunlap ME, Bibevski S, Rosenberry TL and Ernsberger P (2003) Mechanisms of altered vagal control in heart failure: influence of muscarinic receptors and acetylcholinesterase activity. *Am J Physiol Heart Circ Physiol* 285: 1632-40.

Eglen RM and Watson N (1996) Selective muscarinic receptor agonists and antagonists. *Pharmacology & Toxicology 78(2):59-68*.

Fu L-X, Feng Q-P, Liang Q-M, Sun X-Y, Hedner T, Hoebeke J and Hjalmarson A (1993) Hypersensitivity of Gi protein mediated muscarinic receptor adenylyl cyclase in chronic ischaemic heart failure in the rat. *Cardiovascular Research* 27: 2065-70.

Gallo MP, Alloatti G, Carola E, Oberto A and Cesare LR (1993) M_1 muscarinic receptors increase calcium current and phosphoinositide turnover in guinea-pig ventricular cardiocytes. *Journal of Physiology* 471: 41-60.

Giessler C, Dhein S, Ponicke K and Brodde OE (1999) Muscarinic receptors in the failing human heart. *European Journal of Pharmacology* 375: 197-202.

Gullestad L and Madsen S (2004) Moderne diagnostikk og behandling av kronisk hjertesvikt. *Tidsskrift for den Norske Lægeforening* 124: 1107-10.

Haldeman GA, Croft JB, Giles WH and Rashidee A (1999) Hospitalization of patients with heart failure: National hospital discharge survey, 1985 to 1995. *American Heart Journal* 137: 352-60.

Hjalmarson A et al. (1999) Effect of metoprolol CR/XL in chronic heart failure: Metoprolol CR/XL Randomised Intervention Trial in Congestive Heart Failure (MERIT-HF). *Lancet* 353: 2001-7.

Hopkins AL and Groom CR (2002) The druggable genome. *Nat Rev Drug Discov* 1: 727-30.

Hudkins RL, Stubbins JF and DeHaven-Hudkins DL (1993) Caramiphen, iodocaramiphen and nitrocaramiphen are potent, competitive, muscarinic M1 receptor-selective agents. *European Journal of Pharmacology* 231: 485-8.

Hunt SA et al. (2001) ACC/AHA Guidelines for the Evaluation and Management of Chronic Heart Failure in the Adult: Executive Summary A Report of the American College of Cardiology/American Heart Association Task Force on Practice Guidelines (Committee to

Revise the 1995 Guidelines for the Evaluation and Management of Heart Failure). *Circulation* 104: 2996-3007.

Jensen J, Brors O and Dahl HA (1995) Different beta-adrenergic receptor density in different rat skeletal muscle fibre types. *Pharmacology & Toxicology* 76: 380-5.

Kaumann AJ, Engelhardt S, Hein L, Molenaar P and Lohse M (2001) Abolition of (-)-CGP 12177-evoked cardiostimulation in double β_1/β_2-adrenoceptor knockout mice. Obligatory role of β_1-adrenoceptors for putative β_4-adrenoceptor pharmacology. *Naunyn-Schmiedebergs Archives of Pharmacology* 363: 87-93.

Kent KM, Epstein SE, Cooper T and Jacobowitz DM (1974) Cholinergic innervation of the canine and human ventricular conducting system. Anatomic and electrophysiologic correlations. *Circulation* 50: 948-55.

Kilts JD et al. (2000) β_2-Adrenergic and Several Other G Protein-Coupled Receptors in Human Atrial Membranes Activate Both G_s and G_i. *Circ Res* 87: 705-9.

Krejci A and Tucek S (2002) Quantitation of mRNAs for M_1 to M_5 subtypes of muscarinic receptors in rat heart and brain cortex. *Mol Pharmacol* 61: 1267-72.

Le Guludec D, Cohen-Solal A, Delforge J, Delahaye N, Syrota A and Merlet P (1997) Increased Myocardial Muscarinic Receptor Density in Idiopathic Dilated Cardiomyopathy : An In Vivo PET Study. *Circulation* 96: 3416-22.

Loffelholz K and Pappano AJ (1985) The parasympathetic neuroeffector junction of the heart.. *Pharmacological Reviews 37(1):1-24*.

Madsen S (1994) *Hjertesvikt : Årsaker, diagnostikk og behandling*. S. Madsen.

McKinney, M. Current Protocols in Pharmacology. Enna, S. J et al. [1], 1.3.1-1.3.33. 1998. Taylor, G. P.

Mertens MJF, Batink HD, Mathy M-J, Pfaffendorf M and Van Zwieten PA (1995) Reduced muscarinic cholinoceptor density and sensitivity in various models of experimental cardiac hypertrophy. *Journal of Autonomic Pharmacology* 15: 465-74.

Michel MC, Hanft G and Gross G (1994) Radioligand binding studies of alpha1-adrenoceptor subtypes in rat heart. *British Journal of Pharmacology* 111: 533-8.

Mügge A, Reupcke C and Scholz H (1985) Increased myocardial $\alpha_1$adrenoceptor density in rats chronically treated with propranolol. *European Journal of Pharmacology* 112: 249-52.

Myslivecek J, Ricny J, Kolar F and Tucek S (2003a) The effects of hydrocortisone on rat heart muscarinic and adrenergic α_1, β_1 and β_2 receptors, propranolol-resistant binding sites and on some subsequent steps in intracellular signalling. *Naunyn-Schmiedebergs Archives of Pharmacology* 368: 366-76

Myslivecek J and Trojan S (2003b) The importance of the prolonged postnatal period in determination of heart atrial muscarinic receptor and β-adrenoceptor densities. *Life Sci* 73: 3289-96.

Oki T, Yamada S, Tohma A and Kimura R (2001) Muscarinic receptor binding characteristics in rat tissues after oral administration of oxybutynin and propiverine. *Biological & Pharmaceutical Bulletin* 24: 491-5.

Ponicke K, Heinroth-Hoffmann I and Brodde OE (2003) Demonstration of functional M_3-muscarinic receptors in ventricular cardiomyocytes of adult rats. *Br J Pharmacol* 138: 156-60.

Qvigstad, E. Adrenergic and serotonergic receptor functions in the failing heart. 2004. Faculty of Medicine, University of Oslo.

Rang, H. P., Dale, M. M. and Ritter, J. Pharmacology. Fourth, 30-40. 1999.

Remme WJ and Swedberg K (2002) Comprehensive guidelines for the diagnosis and treatment of chronic heart failure: Task force for the diagnosis and treatment of chronic heart failure of the European Society of Cardiology. *European Journal of Heart Failure* 4: 11-22.

Rosenberger LB, Yamamura HI and Roeske WR (1980) Cardiac muscarinic cholinergic receptor binding is regulated by Na^+ and guanyl nucleotides. *J Biol Chem* 255: 820-3.

Rosenthal HE (1967) A graphic method for the determination and presentation of binding parameters in a complex system. *Anal Biochem* 20: 525-32.

Scatchard G (1949) The attractions of proteins for small molecules and ions. *Ann N Y Acad Sci* 51: 660-7.

Sharma VK, Colecraft HM, Rubin LE and Sheu SS (1997) Does mammalian heart contain only the M_2 muscarinic receptor subtype? *Life Sci* 60: 1023-9.

Sharma VK, Colecraft HM, Wang DX, Levey AI, Grigorenko EV, Yeh HH and Sheu SS (1996) Molecular and functional identification of M_1 muscarinic acetylcholine receptors in rat ventricular myocytes. *Circ Res* 79: 86-93.

Sjaastad I, Schiander I, Sjetnan A, Qvigstad E, Bokenes J, Sandnes D, Osnes J-B, Sejersted OM and Skomedal T (2003) Increased contribution of α_1- vs. β-adrenoceptor-mediated inotropic response in rats with congestive heart failure. *Acta Physiologica Scandinavica* 177: 449-58

Sjaastad I, Sejersted OM, Ilebekk A and Bjornerheim R (2000) Echocardiographic criteria for detection of postinfarction congestive heart failure in rats. *J Appl Physiol* 89: 1445-54.

Snyder SH, Chang KJ, Kuhar MJ and Yamamura HI (1975) Biochemical indentification of the mammalian muscarinic cholinergic receptor. *Federation Proceedings 34(10):1915-21.*

Tveit, K. Regulation of G protein coupled receptors involved in congestive heart failure - a quantitative reverse transcriptase polymerase chain reaction study. 2003. MSD Cardiovascular

Research Center, Rikshospitalet University Hospital and Department of Pharmacology, University of Oslo.

Vatner DE, Lee DL, Schwarz KR, Longabaugh JP, Fujii AM, Vatner SF and Homcy CJ (1988) Impaired cardiac muscarinic receptor function in dogs with heart failure. *Journal of Clinical Investigation* 81: 1836-42.

Vatner DE, Sato N, Galper JB and Vatner SF (1996) Physiological and Biochemical Evidence for Coordinate Increases in Muscarinic Receptors and Gi During Pacing-Induced Heart Failure. *Circulation* 94: 102-7.

Wang Z, Shi H and Wang H (2004) Functional M_3 muscarinic acetylcholine receptors in mammalian hearts. *Br J Pharmacol* 142: 395-408.

Willmy-Matthes P, Leineweber K, Wangemann T, Silber RE and Brodde OE (2003) Existence of functional M_3-muscarinic receptors in the human heart. *Naunyn-Schmiedebergs Archives of Pharmacology* 368: 316-9.

Wong SKF (2003) G protein selectivity is regulated by multiple intracellular regions of GPCRs. *NeuroSignals* 12: 1-12.

Xiao RP, Zhu W, Zheng M, Chakir K, Bond R, Lakatta EG and Cheng H (2004) Subtype-specific β-adrenoceptor signaling pathways in the heart and their potential clinical implications. *Trends in Pharmacological Sciences* 25: 358-65.

Yamamura HI and Snyder SH (1974) Muscarinic cholinergic binding in rat brain. *Proceedings of the National Academy of Sciences of the United States of America* 71: 1725-9.

8 APPENDIX

8.1 Materials and recipes

8.1.1 Chemicals and reagents

Chemical/Reagent	Abbreviation	Manifacturer	Cat.no
1,10-phenantroline monohydrate		Sigma	P9375
1,1-Dimethyl-4-diphenylacetoxypiperidinium iodide	4-DAMP	Tocris	0482
11-[[2-[(Diethylamino)methyl]-1-piperidinyl]acetyl]-5,11-dihydro-6*H*-pyrido[2,3-b][1,4]benzodiazepin-6-one	AF-DX 116	Tocris	1105
1-quinacliinyl[phenyl-4^{3}H] benzilate	[^{3}H]QNB	Amersham	TRK 604
2-Diethylaminoethyl 1-(4-nitrophenyl)cyclopentanecarboxylate hydrochloride 11-[[2-[(Diethylamino)methyl]-1-piperidinyl]acetyl]-5,11-dihydro-6*H*-pyrido[2,3-b][1,4]benzodiazepin-6-one	Nitrocaramiphen	Tocris	0469
Absolute ethanol		Arcus	-
Atropine sulfate salt		Sigma	A0257
BCA Protein Assay Kit		Uptima	UP40840A
Carbamoylcholine chloride, carbachol	CCh	Sigma	C4382
dH_2O		-	-
Dimethyl sulfoxide	DMSO	Sigma	D5879
Ethylenedinitrilo tetraacetic acid	EDTA	Merck	8418.0250
Guanosine 5'-[β,γ-imido]triphosphate trisodium salt	Gpp(NH)p	Sigma	G0635
Guanosine 5'-triphosphate sodium salt hydrate	GTP	Sigma	G8877
Hydrochloric acid fuming 37%	HCl	Merck	1.00317.1000
Magnesium chloride hexahydrate	$MgCl \times 6H_2O$	Merck	5833.1000
MicroScint		Packard	6013611
N-Ethyl-3-hydroxy-2-phenyl-*N*-(pyridinylmethyl)propanamide	Tropicamide	Tocris	0909
Opti-fluor		Packard	6013199
Phenylmethanesulfonyl fluorid	PMSF	Sigma	P7626
Polyethyleneimine 50% solution		Sigma	P3143

Potassium chloride	KCl	Merck	1.04936.1000
Sodium chloride	NaCl	Merck	1.06404.0500
Tris(hydroxmetyl)aminomethan	Tris	Merck	1.08382.0500

8.1.2 Content of buffers

Reagent	**Ingredients**
Buffer for tissue preparation and incubation (TME buffer)	50 mmol/L Tris 10 nmol/L $MgCl_2$ x 6 H_2O 1 mmol/L EDTA pH adjusted to 7.4 at room temperature by 2 mol/L HCl
Buffer for tissue preparation (TME buffer with protease inhibitors)	50 mmol/L Tris 10 nmol/L $MgCl_2$ x 6 H_2O 1 mmol/L EDTA 100 µmol/L PMSF 100 µmol/L phenantroline pH adjusted to 7.4 at room temperature by 2 M HCl
Washing buffer	10 mmol/L Tris 2 mmol/L $MgCl_2$ x 6 H_2O pH adjusted to 7.0 at room temperature by hydrochloric acid fuming 37%

8.2 Protocols

8.2.1 Membrane preparation

1. Add a given volume of TME buffer with protease inhibitors, approximately 2/3 of the total volume, into a glass-glass homogeniser on ice.
2. Weigh one part powder of cardiac ventricular tissue in plastic equipment precooled in liquid nitrogen. Transfer immediately the cardiac ventricular tissue into the glass-glass homogeniser. (The amount of cardiac ventricular tissue needed for each experiment has to be calculated based on the final volume of membrane preparation).
3. Add the rest of the TME buffer with protease inhibitors into the glass-glass homogeniser, at a total volume of 19 volumes the weight of the cardiac ventricular tissue.
4. Set the homogeniser, Tri-R Stri-R model S 63 C (Tri-R Instruments, Inc), at level 6, and homogenize the sample by lifting the glass-glass homogeniser up and down 10 times or until the sample is homogenous.
5. Put the glass-glass homogeniser back on ice.
6. Transfer the homogenized membrane preparation to a suitable tube.
7. Add an equal volume of 1 mol/L KCl as the volume of the membrane preparation.
8. Mix the reagents thoroughly with a whirl mixer.
9. Leave the tubes on ice for 10 minutes.
10. Spin the membranes down at 20000 rpm for 12 minutes at 4°C with rotor 20.1 in a Beckman J2-MC Centrifuge (Beckman Instruments, Inc).
11. Put the tube back on ice.
12. Remove the supernatant and resuspend the resulting pellet in 19 volumes the weight of the heart tissue, in TME buffer with protease inhibitors, by using an Ultra-Turrax type TP 18-10 (Ika Werk) at maximum speed. Lift the tube up and down 10 times and keep the tube on ice before repeating another 10 times of lifting the tube up and down.
13. Repeat point 10 –12 twice but resuspend the precipitate in TME buffer instead of TME buffer with protease inhibitors. The last time resuspend in 16 volumes TME buffer instead of 19.
14. Filter the membrane preparation through nylon mesh (pore size: 60 my).

15. Keep the membrane preparation on ice until use.

8.2.2 Incubation

1. Add the different ingredients in a cone bottom 96-well microtiterplate on ice. The reaction mixture in each well is described in table 9 for saturation- and competition experiments and experiments to study if steady state was reached.

Table 9: Incubation mixture in each well in a 96-well microtiterplate in the saturation- and competition experiments and experiment to study the incubation time. All the volumes are given as µL and the ingredients are given in the order loaded to the microtiterplate.

	Saturation binding experiments and experiments to study the incubation time		**Competition binding experiments**	
	Total binding	**Non-specific binding**	**Total binding**	**Non-specific binding**
Incubation buffer (=TME buffer)	175 µL	150 µL	150 µL	150 µL
[^{3}H]QNB	25 µL	25 µL	25 µL	25 µL
Atropine 1 µmol/L (at final concentration)		25 µL		25 µL
Unlabelled ligand			25 µL	
Membrane preparation	50 µL	50 µL	50 µL	50 µL

Saturation binding experiments were performed by eight concentrations of [^{3}H]QNB, 0.06 nmol/L-7.2 nmol/L dissolved in TME buffer. The saturation binding experiments were done in triplets at each concentration.

The experiment to study the incubation time was performed at three critical concentrations of [^{3}H]QNB, 0.056 nmol/L, 0.22 nmol/L and 0.89 nmol/L. The samples were done in triplets at each time point at each concentration of [^{3}H]QNB.

Competition binding experiments were performed with 0.89 nmol/L [^{3}H]QNB and concentrations of unlabelled ligands as described in table 10.

Table 10: Unlabelled ligands, vehicle in stock solutions and concentration range used in competition binding experiments. All the concentrations are given as final concentrations in the assay.

Unlabelled ligand	Vehicle in stock solution	Concentration range
Atropine	dH_2O	9.5 pmol/L – 10 µmol/L
Nitrocaramiphen	dH_2O	0.95 nmol/L – 1 mmol/L
AF-DX 116	DMSO	95 pmol/L – 100 µmol/L
4-DAMP	DMSO	9.5 pmol/L – 10 µmol/L
Tropicamide	DMSO	95 pmol/L – 100 µmol/L
Carbachol	dH_2O	9.5 nmol/L – 10 mmol/L

The experiments were performed by using 21 single concentrations of each unlabelled ligand. Competition binding experiments with carbachol were performed in the absence and the presence of 100 µmol/L GTP, and some additional experiments were performed in the absence and the presence of 100 µmol/L Gpp(NH)p.

2. Cover the microtiterplate with a suitable lid.
3. Carry out the incubation in a waterbath, Grant OLS 2000 (KEBO Lab), at 24°C while shaking the microtiterplate at 30 strokes per minute.
4. Make the incubation last for 120 minutes except in the experiments to study if steady state was reached when the incubation lasts for 90, 120 and 150 minutes.
5. Terminate the incubation by putting the microtiterplate on ice.
6. For each experiment, control the concentration of [^{3}H]QNB by adding 25 µL of each concentration of [^{3}H]QNB to a Nunc-tube, 5 parallels of each concentration.
7. To each Nunc-tube add 50 µL 0.5 mol/L HCl and 1 mL Opti-Fluor.
8. Count the tubes in a Liquid Scintillation Analyser Tri-Carb 2300 TR (Packard Instrument & Co).

8.2.3 Separation of the bound and the free radioligand and measurement of the amount of radioactive ligand bound

1. Presoak a glassfiber filter GF/C plate in 0.3% polyethyleneimine solution.
2. Wash the filter 4 times with 250 µL cold washing buffer in a Packard Cell Harvester (Packard Instrument Co.).
3. Add the reaction mixture to the filters via the cell harvester (Packard Instrument Co.)
4. Wash the GF/C filter plate rapidly 5 times with cold washing buffer.
5. Dry the GF/C filter plate at 37°C for 30 minutes or until the filter is dry.
6. Add 20 µL MicroScint liquid scintillation coctail (Packard Instrument Co.) to each well.
7. Count the GF/C filter plate in a Packard TopCount Scintillation Counter (Packard Instrument Co.)

8.2.4 Protein quantification

1. Add BCA standard in duplets, 20 µL of each, and samples in triplets, 5 µL of each, in a flat bottom 96-well microtiterplate according to figure 19.
2. Add 50 parts of BCA reagent A and one part of BCA reagent B to a tray, mix the reagents and load 250 µL of the solution to each well in the microtiterplate.
3. Cover the microtiterplate with a suitable lid and shake the plate gently for approximately 30 seconds.
4. Incubate the microtiterplate for 30 minutes at 37°C.
5. Let the microtiterplate settle at room temperature.
6. Remove the lid and analyse the samples using a plate spectrophotometer, Bio Assay Reader HTS 7000 (Perkin Elmer), at a wavelength of 570 nm.
7. Ensure that the standard curve follows a linear line. If not, the protein measurement needs to be repeated.

	1	2	3	4	5	6	7	8	9	10	11	12
A	0	0	s1	s1	s1							
B	125	125	s2	s2	s2							
C	250	250	s3	s3	s3							
D	500	500	s4	s4	s4							
E	750	750	s5	s5	s5							
F	1000	1000	s6	s6	s6							
G	1500	1500	s7	s7	s7							
H			s8	s8	s8							

Figure 19: Loading of a 96-well microtiterplate for protein quantification. The standard solutions are added as duplicates, 20 µL in each well, and the concentrations are given as µg/mL. The samples are added as triplicates, 5 µL in each well.